IMES DISCUSSION PAPER SERIES

Wrong-way Risk in Credit Valuation Adjustment of Credit Default Swap with Copulas

Tetsuya Adachi, Takumi Sueshige, and Toshinao Yoshiba

Discussion Paper No. 2019-E-1

IMES

INSTITUTE FOR MONETARY AND ECONOMIC STUDIES

BANK OF JAPAN

2-1-1 NIHONBASHI-HONGOKUCHO
CHUO-KU, TOKYO 103-8660
JAPAN

IMES Discussion Paper Series 2019-E-1
January 2019

Wrong-way Risk in Credit Valuation Adjustment of Credit Default Swap with Copulas

Tetsuya Adachi*, Takumi Sueshige, and Toshinao Yoshiba*****

Abstract

We compare several wrong-way risk models for the credit valuation adjustment of a credit default swap under a copula approach with stochastic default intensities. We show that the tail dependent copulas well capture the wrong-way risk for the credit valuation adjustment. To that end, we employ an affine jump diffusion process for the default intensity to derive the distribution function of the cumulative intensity, based on the copula approach. To reduce computing time, we propose an approximation method using the fractional fast Fourier transform and numerical integration to the characteristic function of the cumulative intensity.

Keywords: Credit valuation adjustment; Credit default swap; Affine jump diffusion; Fractional fast Fourier transform; Characteristic function

JEL classification: G13

* Economist, Institute for Monetary and Economic Studies, Bank of Japan (currently, PwC Consulting LLC, E-mail: tetsuya.adachi@pwc.com)

** Senior, EY Shinnihon LLC (currently, School of Computing, Tokyo Institute of Technology, E-mail: sueshige.t.aa@m.titech.ac.jp)

*** Director and Senior Economist, Institute for Monetary and Economic Studies (currently, Financial System and Bank Examination Department), Bank of Japan (E-mail: toshinao.yoshiba@boj.or.jp)

The authors would like to thank Rüdiger Frey (Vienna University), Masayasu Kanno (Nihon University), Yukio Muromachi (Tokyo Metropolitan University), Hidetoshi Nakagawa (Hitotsubashi University), Takashi Ohmoto (Nomura Asset Management), Yuji Sakurai (Federal Reserve Bank of Richmond), participants at the RIMS Workshop on Financial Modeling and Analysis and the 10th International Conference on Computational and Financial Econometrics, and the staff at the Institute for Monetary and Economic Studies of the Bank of Japan for their useful comments and discussions. The views expressed in this paper are those of the authors and do not necessarily reflect the official views of the Bank of Japan.

1. Introduction

During the global financial crisis of 2007–08, financial institutions suffered from massive loss due to the realization of wrong-way risk (WWR).[1] Since then, WWR has been recognized as an important risk to be considered by financial institutions, and has been taken into account for pricing and risk management of credit valuation adjustment (CVA) by advanced financial institutions. In addition, the Basel Committee on Banking Supervision (BCBS) requires the regulatory CVA to capture a significant level of adverse dependence between exposure and the counterparty's credit quality; that is, WWR (BCBS, 2017). In response to those demands in pricing, risk management and regulation, various types of WWR models have been developed, however, there is no consensus how to model and measure it. In this paper, we propose some modeling methodologies of WWR in CVA pricing and use credit default swap (CDS) as a typical instrument having large impact of WWR.

Against the background, Brigo and Chourdakis (2009) and Brigo and Capponi (2010) employ the Gaussian copula to capture the positive dependence between the credit quality of the counterparty and that of the reference name. However, the Gaussian copula often becomes the focus of the criticism due to i) the unrealistic dependence between credit qualities as pointed out by Lee and Capriotti (2015) and ii) the underestimation of CVA stemming from its weak tail dependence as pointed out by Glasserman and Yang (2018).

We therefore compare the unilateral CVA with WWR on a CDS using four well known copulas, namely the Gaussian, Student's *t*, Clayton, and survival Gumbel copulas, under the same strength of copula-correlation parameter. In results, the tail dependent copulas including the Student's *t*, survival Gumbel, and Clayton copulas capture the WWR in the CVA better than the Gaussian copula does as pointed out by Glasserman and Yang (2018). In addition, we find that the impact of CVA with WWR depends on the employed copula and the copula-correlation parameter. When the copula-correlation parameter is small, the Student's *t* copula yields larger CVA than other copulas do. When it is large, the Clayton and survival Gumbel copulas yield larger CVA. It reflects that the Student's *t* copula does not reduce to the independent copula even when the copula-correlation parameter is zero. This characteristic disappears as the copula-correlation parameter becomes large due to the strong tail-dependence of the Clayton and survival Gumbel copulas.

---

[1] Wrong-way risk arises when an adverse relationship between exposure to a counterparty and the credit quality of that counterparty triggers large loss in portfolios.

Other than copulas, jump factors are intensively studied to capture the credit dependence for modeling WWR as Jarrow, Lando, and Yu (2005) stress the necessity of the jump element to represent the risk premium in a credit spread. Leung and Kwok (2005) study counterparty risk using a deterministic intensity with jump triggered by the default of other companies. Mercurio and Li (2015) assume a price jump of reference asset at the event of counterparty default. Bo and Capponi (2014) show an explicit formula of a bilateral CVA on a portfolio consisting of an asymptotically large number of CDSs assuming a stochastic default intensity model with a common and an independent jump. Adachi and Uchida (2015) reveal the mechanism of booms and busts of asset prices via transitions between two different types of traders with and without managing WWR derived from a common jump embedded in two risk factors.

Copulas are also independently employed to capture wider credit dependences. Cherubini (2013) represents the WWR in CVA of an interest rate swap by a co-monotonic copula between default probabilities and cumulative distribution of interest rates. He proposes the CVA as the weighted average of that from the co-monotonic copula and that from the independent copula, which is partially corrected by Černý and Witzany (2018). Brigo and Chourdakis (2009) and Brigo and Capponi (2010) introduce the Gaussian copula into a stochastic default intensity process without jump. Rosen and Saunders (2012) capture the WWR using the Gaussian copula between an empirical distribution of market factor and cumulative default probabilities. Lee and Capriotti (2015) extend the copula approach to compute the CVA of CDS portfolio by employing the Clayton copula. They mention that the Clayton copula produces more realistic dependence of the default intensity dynamics conditional on the counterparty default than the Gaussian copula. Glasserman and Yang (2018) also show the Gaussian copula could underestimate CVA. Böcker and Brunnbauer (2014) propose general copula approach to capture the potential future exposure for CVA with WWR and apply the method to the Gaussian, Clayton, Frank, and Gumbel copulas.

Based on the model of Brigo and Chourdakis (2009) and Brigo and Capponi (2010), we extend their model of the Gaussian copula to other tail dependent copulas including the Student's *t* ,Clayton, and survival Gumbel copulas as well as adding a jump factor to the stochastic intensity process. Brigo and El-Bachir (2010) call the process as the shifted square root jump diffusion (SSRJD). Since SSRJD is an affine jump diffusion process, the characteristic function of SSRJD cumulative intensity is analytically solvable. In theory, applying the Fourier inversion and numerical integration to the characteristic function, the CDF of the cumulative default intensity can be obtained. However, the complex-valued characteristic function including log function is multivalued and undefined. The derivation of the characteristic function is not straightforward. To handle this problem, we define the characteristic function of cumulative SSRJD on a single-layered Riemann surface. To reduce the computational cost of the Fourier inversion, we employ the fractional Fourier transform in Bailey and Swarztrauber (1991) and Chourdakis (2004).

This paper is organized as follows. Section 2 overviews the copula approach for the default intensity model and shows the numerical comparison with Gaussian, Student's *t*, Clayton, and survival Gumbel copula approaches and non-copula approaches. Section 3 derives the conditional survival probabilities with SSRJD default intensities. Section 4 gives concluding remarks.

2. Copula approach with SSRJD default intensity

This section describes how the CVA of CDS is calculated in a copula approach using a default intensity model. The calculation in a copula approach requires the distribution function of the cumulative intensity. We analyze the CVA of CDS comparing the models with no wrong-way risk, no jump in default intensities, and non-copula approaches.

2.1. Valuation of CVA of CDS

We consider a CDS contract between Bank *A* (protection buyer) and Bank *C* (protection seller) whose reference entity is Firm *R*. Bank *A* is assumed to be default-free. The maturity of the contract is t_m and Bank *A* pays a premium with the rate sp_R to the bank *C* at t_j $(j = 1, \dots, m)$ until Firm *R* defaults with the equal interval, $\Delta = t_j - t_{j-1}$ $(\forall j)$. In this paper, the premium payment is assumed to be monthly, $\Delta = 1/12$. We refer to Bank *C* and Firm *R* using $k = C, R$.

For the valuation, if Firm *R* defaults at time $\tau_R \in (t_{j-1}, t_j]$, the default is assumed to happen at time t_j and the Bank *A* is assumed to pay a premium to Bank *C* at time t_j. The loss rate given the default of Bank *C* and the reference Firm *R* are given by LGD_C and LGD_R, respectively. Both are assumed to be constant. The value of the CDS of the notional amount NA without CVA at time t_j is given by

$$V_{CDS}^{No\,CVA}(t_j) = \left(\mathrm{LGD}_R\, \mathbb{E}_j^{\mathbb{Q}}\left[DF(t_j, \tau_R) 1_{\{\tau_R \in (t_j, t_m]\}}\right] - sp_R \Delta \sum_{l=j+1}^{m} DF(t_j, t_l) \mathbb{E}_j^{\mathbb{Q}}\left[1_{\{\tau_R > t_{l-1}\}}\right] \right) \times NA, \tag{1}$$

where $\mathbb{E}_j^{\mathbb{Q}}[\cdot]$ is the expectation operator at time t_j under the risk neutral probability $\mathbb{Q}$. $DF(t_j, t_i)$ denotes the discounting factor from t_j to t_i under the probability $\mathbb{Q}$. In this paper, we assume the OIS (overnight index swap) discounting factor on May 1, 2008 with quarterly premium legs. Evaluating equation (1) by discretizing at time t_l $(l = j+1, \dots, m)$,

$$V_{CDS}^{No\,CVA}(t_j) = NA \sum_{l=j+1}^{m} DF(t_j, t_l)\{\mathrm{LGD}_R PD_{R,j}(t_{l-1}, t_l) - sp_R \Delta\left(1 - PD_{R,j}(t_j, t_{l-1})\right)\}, \tag{2}$$

where $PD_{R,j}(t_{l-1}, t_l)$ denotes the term default probability measure at time t_j that the reference Firm R defaults during the term $(t_{l-1}, t_l]$, that is, $PD_{R,j}(t_{l-1}, t_l) = \mathbb{E}_j^{\mathbb{Q}}[1_{\{\tau_R \in (t_{l-1}, t_l]\}} | \tau_R > t_j] = \mathbb{Q}(\tau_R > t_{l-1} | \tau_R > t_j) - \mathbb{Q}(\tau_R > t_l | \tau_R > t_j)$.

The unilateral CVA observed from Bank A at time t_0 is calculated by

$$CVA_A(t_0) = \mathrm{LGD}_C \sum_{j=1}^{m} DF(t_0, t_j)\, \mathbb{E}_0^{\mathbb{Q}}\left[V_{CDS}^{No\,CVA}(t_j)^+ \middle| \tau_C \in (t_{j-1}, t_j]\right] PD_{C,0}(t_{j-1}, t_j), \tag{3}$$

where $V^+ \equiv \max(V, 0)$. $PD_{C,0}(t_{j-1}, t_j)$ denotes the term default probability measure at time t_0 that the counterparty bank C defaults during the term $(t_{j-1}, t_j]$, that is, $PD_{C,0}(t_{j-1}, t_j) = \mathbb{E}_0^{\mathbb{Q}}\left[1_{\{\tau_C \in (t_{j-1}, t_j]\}}\right] = \mathbb{Q}(\tau_C > t_{j-1}) - \mathbb{Q}(\tau_C > t_j)$.

The key point to capture WWR is modeling the conditional expected exposure with the counterparty default, $\mathbb{E}_0^{\mathbb{Q}}\left[V_{CDS}^{No\,CVA}(t_j)^+ \middle| \tau_C \in (t_{j-1}, t_j]\right]$, becomes larger than the unconditional one, $\mathbb{E}_0^{\mathbb{Q}}\left[V_{CDS}^{No\,CVA}(t_j)^+\right]$.

We evaluate the unilateral CVA observed from Bank A at time t_0 by simulation with N paths. Denoting the default time of the Bank C and the reference Firm R with i-th path by $\tau_C^{(i)}$ and $\tau_R^{(i)}$respectively, the CVA is calculated by

$$CVA_A(t_0) = \frac{\mathrm{LGD}_C}{N} \sum_{i=1}^{N} \sum_{j=1}^{m} DF(t_0, t_j) V_{CDS}^{No\,CVA}(t_j)^+ 1_{\left\{\tau_C^{(i)} \in (t_{j-1}, t_j], \tau_R^{(i)} \geq \tau_C^{(i)}\right\}}. \tag{4}$$

2.2. Default intensity model with simultaneous jump

Although Brigo and Chourdakis (2009) and Brigo and Capponi (2010) use shifted square root diffusion without jump (SSRD), Jarrow, Lando, and Yu (2005) indicate that the jump element is important for the risk premium in the credit spread. Duffie and Gârleanu (2001), Brigo and El-Bachir (2010), and others adopt the SSRJD for the stochastic default intensity. Therefore, we introduce the stochastic default intensity with jump.

The default times τ_C and τ_R are modeled by the default intensities $\lambda_C(t)$ and $\lambda_R(t)$, respectively. Brigo and Chourdakis (2009) adopt the following square root diffusion (SRD) for the default intensity $\lambda_k(t)$ $(k = C, R)$ as

$$d\lambda_k(t) = \kappa_k\big(\theta_k - \lambda_k(t)\big)dt + \sigma_k\sqrt{\lambda_k(t)}dW_k(t), \tag{5}$$

where $W_k(t)$s $(k = C, R)$ are the Brownian motions which have constant correlation as

$$d\langle W_C, W_R\rangle(t) = \rho_{C,R}dt. \tag{6}$$

For the valuation of the term default probabilities and the survival probabilities in equations (2) and (3), Brigo and Chourdakis (2009) incorporate the adjusting elements $\Psi_k(t_j)$ by the market calibration. Hence, the stochastic process of the default intensity $\lambda_k(t)$ $(k = C, R)$ is called Shifted SRD.

We assume the upshifted default intensity $\lambda_k(t)$ $(k = C, R)$ with the following square root jump diffusion (SRJD).

$$d\lambda_k(t) = \kappa_k\big(\theta_k - \lambda_k(t)\big)dt + \sigma_k\sqrt{\lambda_k(t)}dW_k(t) + dJ_k(t), \tag{7}$$

where $J_k(t)$ is the jump component using marked Poisson process $N^\eta(\boldsymbol{z}, t)$ with the intensity η as

$$J_k(t) = \int_{t_0}^{t_0+t}\int_{\mathbb{R}^+} z_k dN^\eta(\boldsymbol{z}, s), \qquad \boldsymbol{z} = (z_C, z_R), \qquad z_k \sim \mathrm{Exp}(\zeta_k). \tag{8}$$

The timing of the jump is common to each default intensity. Each default intensity has each jump size mean ζ_k. Regarding the correlation of each jump size, we consider two types: (i) simultaneous comonotone jump, that is, the jump size z_k is given as $z_k = \zeta_k z$ with the common exponential random number $z \sim \mathrm{Exp}(1)$, and (ii) simultaneous independent jump, that is, the jump sizes z_C and z_R are given as $z_C \sim \mathrm{Exp}(\zeta_C)$ and $z_R \sim \mathrm{Exp}(\zeta_R)$ independently. The diffusion parts have a constant correlation as

$$d\langle W_C, W_R\rangle(t) = \rho_{C,R}^{jump}dt. \tag{9}$$

For the valuation of the term default probabilities and the survival probabilities in equations (2) and (3), we also incorporate the adjusting elements $\Psi_k(t_j)$ by the market calibration described in Section 2.5.

For the discretized CVA valuation (3), we assume constant default intensity between the discretized time, $\lambda_k(t) = \bar{\lambda}_{k,j}$ for $t \in (t_{j-1}, t_j]$, to identify the default time of counterparty τ_C and whether the reference firm survives at time τ_C, $\tau_R > \tau_C$. If $\tau_C \in (t_{j-1}, t_j]$ and $\tau_R > \tau_C$, the conditional survival probability $\mathbb{Q}(\tau_R > t_l | \tau_R > t_j)$ is calculated analytically in the SSRJD default intensity (see Section 3.1).

2.3. Copula approach for cumulative intensity

The copula approach shown in Brigo and Chourdakis (2009) represents WWR by connecting the cumulative default probability of the counterparty U_C to that of the reference firm U_R with the copula function:

$$C_{C,R}(u_C, u_R) \coloneqq \mathbb{Q}(U_C \le u_C, U_R \le u_R). \tag{10}$$

As the canonical construction of the time of default τ_k $(k = C, R)$ indicated in Bielecki, Jeanblanc, and Rutkowski (2009), the time of default τ_k is connected though an increasing and continuous process of the cumulative default intensity $\Lambda_k(t)$ $(k = C, R)$:

$$\Lambda_k(t) \coloneqq \int_{t_0}^{t} \lambda_k(s) ds\,. \tag{11}$$

The cumulative default probability U_k until the time of default τ_k is given as

$$U_k = 1 - \exp\{-\Lambda_k(\tau_k)\}. \tag{12}$$

Conversely, the time of default τ_k is given as

$$\tau_k = \inf\{t > t_0 | \Lambda_k(t) \ge -\ln(1 - U_k)\}. \tag{13}$$

Given the counterparty defaults at time $\tau_C \in (t_{j-1}, t_j]$ and the reference firm survives until t_j, the survival probability of the reference firm beyond $t \ge t_j$, $\mathbb{Q}(\tau_R > t | \tau_C \in (t_{j-1}, t_j])$, is transformed as:

$$\begin{aligned}
&\mathbb{Q}\left(\tau_R > t \middle| \tau_C \in \left(t_{j-1}, t_j\right]\right) \\
&= \mathbb{Q}\left(1 - e^{-\Lambda_R(\tau_R)} > 1 - e^{-\Lambda_R(t)} \middle| \tau_C \in \left(t_{j-1}, t_j\right]\right) \\
&= \mathbb{Q}\left(\Lambda_R(t) - \Lambda_R(\tau_C) < -\log(1 - U_R) - \Lambda_R(\tau_C) \middle| \tau_C \in \left(t_{j-1}, t_j\right]\right) \\
&= \int_{U_{R|C}}^{1} F_{\Lambda_R(t) - \Lambda_R(\tau_C)}\left(-\log(1 - U_R) - \Lambda_R(\tau_C)\right)\, d\mathbb{Q}\left(U_R \in du_R \middle| \tau_C \in \left(t_{j-1}, t_j\right]\right) \qquad (14) \\
&= \int_{U_{R|C}}^{1} F_{\Lambda_R(t) - \Lambda_R(\tau_C)}\left(\log \frac{1 - U_{R|C}}{1 - U_R}\right) d\mathbb{Q}\left(U_R \in du_R \middle| \tau_C \in \left(t_{j-1}, t_j\right]\right),
\end{aligned}$$

where $F_{\Lambda_R(t) - \Lambda_R(\tau_C)}(\cdot)$ denotes the cumulative distribution function of $\Lambda_R(t) - \Lambda_R(\tau_C)$ and

$$U_{R|C} \coloneqq 1 - \exp\{-\Lambda_R(\tau_C)\}. \tag{15}$$

At the last term in equation (14), $\mathbb{Q}\left(U_R \in du_R \middle| \tau_C \in \left(t_{j-1}, t_j\right]\right)$ is evaluated as:

$$
\begin{aligned}
\mathbb{Q}\left(U_R \in du_R \middle| \tau_C \in \left(t_{j-1}, t_j\right]\right) &= \frac{\mathbb{Q}\left(U_R \in \left(U_{R|C}, U_{R|C} + du_R\right], U_C \in \left(U_{C,j-1}, U_{C,j}\right]\right)}{\mathbb{Q}\left(U_R > U_{R|C}, U_C \in \left(U_{C,j-1}, U_{C,j}\right]\right)} \\
&= \frac{\mathbb{Q}\left(U_R \le U_{R|C} + du_R, U_C \in \left(U_{C,j-1}, U_{C,j}\right]\right) - \mathbb{Q}\left(U_R \le U_{R|C}, U_C \in \left(U_{C,j-1}, U_{C,j}\right]\right)}{1 - \mathbb{Q}\left(U_R \le U_{R|C}, U_C \in \left(U_{C,j-1}, U_{C,j}\right]\right)},
\end{aligned}
\tag{16}
$$

where $U_{C,j} \coloneqq 1 - \exp\left\{-\Lambda_C\left(t_j\right)\right\}$. The conditional distribution function (16) is represented as $C_{R|C}\left(U_{R|C} + du_R; U_C\right)$, where

$$
C_{R|C}(u_R; U_C) \coloneqq \frac{\left.\dfrac{\partial C_{C,R}(u_C, u_R)}{\partial u_C}\right|_{u_C = U_C} - \left.\dfrac{\partial C_{C,R}\left(u_C, U_{R|C}\right)}{\partial u_C}\right|_{u_C = U_C}}{1 - \left.\dfrac{\partial C_{C,R}\left(u_C, U_{R|C}\right)}{\partial u_C}\right|_{u_C = U_C}}. \tag{17}
$$

Using equation (17), equation (14) is represented as:

$$
\begin{aligned}
&\mathbb{Q}\left(\tau_R > t \middle| \tau_C \in \left(t_{j-1}, t_j\right]\right) \\
&= \int_{U_{R|C}}^{1} F_{\Lambda_R(t) - \Lambda_R(\tau_C)}\left(\log \frac{1 - U_{R|C}}{1 - u_R}\right) dC_{R|C}(u_R; U_C).
\end{aligned}
\tag{18}
$$

In equation (18), $F_{\Lambda_R(t) - \Lambda_R(\tau_C)}(\cdot)$ is calculated by numerical integration of the density, which is calculated by Fourier inversion of the characteristic function. We discuss the procedures in Section 3.

2.4. Copulas and their derivatives

While Brigo and Chourdakis (2009) and Brigo and Capponi (2010) adopt a Gaussian copula for the approach, Lee and Capriotti (2015) adopt a Clayton copula for the approach where each default intensity has the Black and Karasinski process (1991). Lee and Capriotti (2015) mention that the Clayton copula produces a more realistic dependence of the default intensity dynamics conditional on the counterparty default, citing Schönbucher and Schubert (2001). After the GFC (global financial crisis) around 2008, much criticism arose for CDO (collateralized debt obligation) rating using the Gaussian copula, which has no tail dependence. Some advanced financial institutions use the Student's *t* copula to evaluate credit portfolio risk or enterprise risk with some risk categories. In light of these discussions, we present not only the Gaussian copula, but also the Student's *t*, Clayton, and survival Gumbel copulas for the default intensity dynamics.

Following Brigo and Chourdakis (2009), we first adopt the Gaussian copula for the copula approach. The bivariate Gaussian copula is given as

$$C^G(u_1, u_2; \rho) \coloneqq \Phi_2(\Phi^{-1}(u_1), \Phi^{-1}(u_2); \rho), \tag{19}$$

where ρ is the copula-correlation parameter, $\Phi_2(\cdot,\cdot;\rho)$ is the bivariate standard Gaussian CDF with the correlation ρ given as equation (20), and $\Phi(\cdot)$ is the univariate standard Gaussian CDF given as equation (21).

$$\begin{aligned} \Phi_2(h, k; \rho) &\coloneqq \int_{-\infty}^{h}\int_{-\infty}^{k} \frac{1}{2\pi\sqrt{1-\rho^2}} \exp\left\{-\frac{x^2 - 2\rho xy + y^2}{2(1-\rho^2)}\right\} dxdy \\ &= \int_{-\infty}^{h} \Phi\left(\frac{k-\rho x}{\sqrt{1-\rho^2}}\right) \frac{1}{\sqrt{2\pi}} \exp\left\{-\frac{x^2}{2}\right\} dx, \end{aligned} \tag{20}$$

$$\Phi(k) \coloneqq \int_{-\infty}^{k} \frac{1}{\sqrt{2\pi}} \exp\left\{-\frac{y^2}{2}\right\} dy. \tag{21}$$

The Kendall's tau, one of the scale-invariant measures of association, is given as:

$$\tau_K^G = \frac{2}{\pi} \arcsin \rho \,. \tag{22}$$

The partial derivative in equation (17) is given as equation (23).

$$\frac{\partial C^G(u_C, u_R; \rho)}{\partial u_C} = \Phi\left(\frac{\Phi^{-1}(u_R) - \rho\Phi^{-1}(u_C)}{\sqrt{1-\rho^2}}\right). \tag{23}$$

For the comparison between copulas, we also adopt the Student's *t* copula for the copula approach. The bivariate Student's *t* copula is given as

$$C^t(u_1, u_2; \rho, \nu) \coloneqq t_{2,\nu}(t_\nu^{-1}(u_1), t_\nu^{-1}(u_2); \rho), \tag{24}$$

where $t_{2,\nu}(\cdot,\cdot;\rho)$ is the bivariate Student's *t* CDF with the copula-correlation ρ given as equation (25), and $t_\nu(\cdot)$ is the univariate Student's *t* CDF given as equation (26).

$$t_{2,\nu}(h, k; \rho) \coloneqq \int_{-\infty}^{h} \frac{1}{2\pi\sqrt{1-\rho^2}} \int_{-\infty}^{k} \left(1 + \frac{x^2 - 2\rho xy + y^2}{\nu(1-\rho^2)}\right)^{-\frac{(\nu+2)}{2}} dxdy, \tag{25}$$

$$t_\nu(h) \coloneqq \frac{\Gamma((\nu+1)/2)}{\Gamma(\nu/2)\sqrt{\pi\nu}} \int_{-\infty}^{h} \left(1 + \frac{x^2}{\nu}\right)^{-\frac{(\nu+1)}{2}} dx \tag{26}$$

The Kendall's tau of the Student's *t* copula is the same as that of the Gaussian copula given as equation (22). The partial derivative in equation (17) is given as

$$
\begin{aligned}
\frac{\partial C^t(u_C, u_R; \rho)}{\partial u_C} &= \frac{\Gamma((\nu+2)/2)}{\Gamma((\nu+1)/2)\sqrt{\pi\nu}\sqrt{1-\rho^2}} \left(1+\frac{x^2}{\nu}\right)^{\frac{(\nu+1)}{2}} \\
&\times \int_{-\infty}^{t_\nu^{-1}(u_R)} \left(1+\frac{x^2-2\rho xy+y^2}{\nu(1-\rho^2)}\right)^{-\frac{(\nu+2)}{2}} dy \\
&= \frac{\Gamma((\nu+2)/2)}{\Gamma((\nu+1)/2)\sqrt{\pi(\nu+1)}} \int_{-\infty}^{\bar{z}} \left(1+\frac{z^2}{\nu+1}\right)^{-\frac{(\nu+2)}{2}} dz,
\end{aligned} \tag{27}
$$

with

$$
\bar{z} := \sqrt{\frac{\nu+1}{\nu+x^2}} \left\{\frac{t_\nu^{-1}(u_R)-\rho x}{\sqrt{1-\rho^2}}\right\}, \qquad x = t_\nu^{-1}(u_C). \tag{28}
$$

Thus the partial derivative in equation (17) is given as

$$
\frac{\partial C^t(u_C, u_R; \rho)}{\partial u_C} = t_{\nu+1}\left(\sqrt{\frac{\nu+1}{\nu+t_\nu^{-1}(u_C)^2}} \left\{\frac{t_\nu^{-1}(u_R)-\rho t_\nu^{-1}(u_C)}{\sqrt{1-\rho^2}}\right\}\right). \tag{29}
$$

Following Lee and Capriotti (2015), we also consider the Clayton copula for comparison. The bivariate Clayton copula is given as

$$
C^C(u_1, u_2; \alpha) := (u_1^{-\alpha} + u_2^{-\alpha} - 1)^{-1/\alpha}. \tag{30}
$$

The Kendall's tau is given as

$$
\tau_K^C = \frac{\alpha}{\alpha+2}. \tag{31}
$$

Equating (22) with (31), the parameter α is given as

$$
\alpha = \frac{4\arcsin\rho}{\pi - 2\arcsin\rho}. \tag{32}
$$

The partial derivative in equation (17) is given as

$$
\frac{\partial C^C(u_C, u_R; \alpha)}{\partial u_C} = u_C^{-\alpha-1}(u_C^{-\alpha} + u_R^{-\alpha} - 1)^{-1/\alpha-1}. \tag{33}
$$

We also consider the survival Gumbel copula for comparison, which comes from an extreme value copula, the Gumbel copula. The bivariate Gumbel copula is given as

$$
C^{Gu}(u_1, u_2; \gamma) := \exp\left\{-((-\log u_1)^\gamma + (-\log u_2)^\gamma)^{1/\gamma}\right\}. \tag{34}
$$

The Kendall's tau is given as

$$
\tau_K^{Gu} = 1 - \frac{1}{\gamma}. \tag{35}
$$

Equating (22) with (35), the parameter γ is given as

$$\gamma = \frac{\pi}{\pi - 2\arcsin\rho}. \tag{36}$$

Since the survival bivariate Gumbel copula is given as

$$C^{SGu}(u_1, u_2; \gamma) = u_1 + u_2 - 1 + C^{Gu}(1 - u_1, 1 - u_2; \gamma), \tag{37}$$

the partial derivative in equation (17) is given as

$$\begin{aligned}\frac{\partial C^{SGu}(u_C, u_R; \gamma)}{\partial u_C} &= 1 - \exp\left\{-((-\log(1-u_C))^{\gamma} + (-\log(1-u_R))^{\gamma})^{1/\gamma}\right\} \\ &\times \{(-\log(1-u_C))^{\gamma} + (-\log(1-u_R))^{\gamma}\}^{1/\gamma - 1} \\ &\times \frac{(-\log(1-u_C))^{\gamma-1}}{1-u_C}.\end{aligned} \tag{38}$$

The Kendall's tau of the survival Gumbel copula is the same as that of the Gumbel copula, given as equation (35).

Table 1 summarizes the parameters, Kendall's tau τ_K, and lower tail dependence λ_L for the bivariate copulas used in this subsection. The lower tail dependence λ_L is given as:

$$\lambda_L = \lim_{u \to 0} \frac{C(u, u)}{u}. \tag{39}$$

Table 1 Bivariate parametric copulas, their Kendall's tau, and lower tail dependence

Copula	Parameter	Kendall's tau τ_K	Lower tail dependence λ_L
Gaussian	ρ	$(2/\pi)\arcsin\rho$	0
Student's *t*	ρ, ν	$(2/\pi)\arcsin\rho$	$2t_{\nu+1}\left(-\sqrt{\frac{(1-\rho)(\nu+1)}{1+\rho}}\right)$
Clayton	α	$\alpha/(\alpha+2)$	$2^{-1/\alpha}$
Survival Gumbel	γ	$1 - 1/\gamma$	$2 - 2^{1/\gamma}$

2.5. Calibration

The parameters in equation (7) of the default intensities $\lambda_C(t)$ and $\lambda_R(t)$ are calibrated from market quotes of CDS in two steps. First, the nonparametric implied survival probabilities $\widehat{\mathbb{Q}}(\tau_k > t_j)$ $(k = C, R)$ are derived from the market quotes. Second, the parameters of each intensity $\lambda_k(t)$ $(k = C, R)$ are calibrated from the nonparametric implied survival probabilities $\widehat{\mathbb{Q}}(\tau_k > t_j)$ $(j = 1, \ldots, m)$.

2.5.1. Implied survival probability

Following Brigo and Capponi (2010), we also apply CDS market quotes on May 1, 2008 of Lehman Brothers (Bank *C*) and Royal Dutch Shell (Firm *R*). The terms of market quotes are given for each year from one year to ten years given as Table 2. Let $t_{b_1}, t_{b_2}, \ldots$ be the maturities of market quotes. In this paper, $\left(t_{b_1}, t_{b_2}, \ldots, t_{b_{10}}\right) = (1,2,\ldots,10)$. The nonparametric implied survival probabilities $\widehat{\mathbb{Q}}(\tau_k > t_{b_l})$ is given by assuming piecewise linear default intensity $\lambda_k(t) = \bar{\lambda}_{k,l}^0 + \bar{\lambda}_{k,l}^1 t$ between the maturities of market quotes $t \in (t_{b_{l-1}}, t_{b_l}]$, as in Brigo and Mercurio (2006) and Brigo and Capponi (2010).

Table 2 CDS market quotes (bp) on May 1, 2008

	1Y	2Y	3Y	4Y	5Y	6Y	7Y	8Y	9Y	10Y
Bank C	203	188.5	166.75	152.25	145	136.3	130	125.8	122.6	120
Firm R	24	24.6	26.4	28.5	30	32.1	33.6	35.1	36.3	37.2

For the calibration, we assume quarterly premium payments and apply CDS market valuation (2) for the firm *R* of the maturity t_m to CDS market quotes for the firms $k = C, R$ of the maturities $t_b = t_{b_1}, t_{b_2}, \ldots, t_{b_{10}}$. The CDS market quote for the firm k of the maturity t_{b_l} observed at time t_0 is denoted as $V_{CDS,k}^{No\ CVA}\left(t_0, t_b; \left(\bar{\lambda}_{k,1}^0, \bar{\lambda}_{k,1}^1\right), \ldots, \left(\bar{\lambda}_{k,l}^0, \bar{\lambda}_{k,l}^1\right)\right)$, where $\left(\bar{\lambda}_{k,l}^0, \bar{\lambda}_{k,l}^1\right)$ are the implied coefficients of the piecewise linear default intensity during $t \in (t_{b_{l-1}}, t_{b_l}]$. We orderly solve

$$
\begin{gathered}
V_{CDS,k}^{No\ CVA}\left(t_0, t_{b_1}; \left(\bar{\lambda}_{k,1}^0, \bar{\lambda}_{k,1}^1\right)\right) = 0, \\
\vdots \\
V_{CDS,k}^{No\ CVA}\left(t_0, t_{10}; \left(\bar{\lambda}_{k,1}^0, \bar{\lambda}_{k,1}^1\right), \ldots, \left(\bar{\lambda}_{k,10}^0, \bar{\lambda}_{k,10}^1\right)\right) = 0,
\end{gathered}
\tag{40}
$$

to obtain the implied coefficients, $\left(\bar{\lambda}_{k,1}^0, \bar{\lambda}_{k,1}^1\right), \ldots, \left(\bar{\lambda}_{k,10}^0, \bar{\lambda}_{k,10}^1\right)$. The implied survival probabilities $\widehat{\mathbb{Q}}(\tau_k > t_{b_l})$ are orderly given as

$$
\begin{gathered}
\widehat{\mathbb{Q}}(\tau_k > t_{b_1}) = \exp\left(-\left(\bar{\lambda}_{k,1}^0 + \bar{\lambda}_{k,1}^1 (t_0 + t_{b_1})/2\right)\left(t_{b_1} - t_0\right)\right), \\
\vdots \\
\widehat{\mathbb{Q}}\left(\tau_k > t_{b_{10}}\right) = \widehat{\mathbb{Q}}\left(\tau_k > t_{b_9}\right) \exp\left(-\left(\bar{\lambda}_{k,10}^0 + \bar{\lambda}_{k,10}^1\left(t_{b_9} + t_{b_{10}}\right)/2\right)\left(t_{b_{10}} - t_{b_9}\right)\right).
\end{gathered}
\tag{41}
$$

2.5.2. Calibration of parameters of SSRD

We first calibrate parameters $\boldsymbol{\beta}_k = (\kappa_k, \theta_k, \sigma_k, \lambda_k(0))$ of SSRD intensity without jump (5) for comparison by equating the theoretical survival probabilities (55) excluding $\alpha_J(s,t)$ term with the implied survival probabilities (41) as the following steps.

1. For $b = b_1, \dots, b_{10}$, calculate
$$\psi(t_b, \boldsymbol{\beta}_k) = \log\left(\widehat{\mathbb{Q}}(\tau_k > t_b)\right) - \log\left(\mathbb{Q}(\tau_k > t_b)\right), \tag{42}$$
where the theoretical survival probability $\mathbb{Q}(\tau_k > t_b)$ is calculated using current parameters for SSRD.

2. Repeat Step 1 to minimize $\Psi\left(t_{b_{10}}, \boldsymbol{\beta}_k\right) = \sum_{i=1}^{10} \psi\left(t_{b_i}, \boldsymbol{\beta}_k\right)^2$ with the constraints $\psi(t_b, \boldsymbol{\beta}_k) \geq 0$ for all $b = b_1, \dots, b_{10}$ and $2\kappa_k\theta_k > \sigma_k^2$.

The calibrated parameters of SSRD intensity are given in Table 3.

Table 3 Calibration SSRD default intensity

k	κ_k	θ_k	σ_k	$\lambda_k(0)$
Bank C	0.5667	0.0155	0.1327	0.0394
Firm R	0.4884	0.0068	0.0100	0.0021

2.5.3. Calibration of parameters of SSRJD

As indicated in Brigo, Morini, and Pallavicini (2013), it is difficult to jointly identify the volatility parameter σ_k and the jump parameters, η and ν_k for the SSRJD intensity (7). Following Brigo, Morini, and Pallavicini (2013), we first set jump parameters, η and ν_k, exogenously before the calibration of the parameters $\boldsymbol{\beta}_k = (\kappa_k, \theta_k, \sigma_k, \lambda_k(0), \zeta_k, \eta)$ of SSRJD intensity (7). The calibration is given as the following steps.

1. Set η and ζ_k exogenously, as $\zeta_k = 0.05$ and $\eta = 0.01$ (simultaneous comonotone jump) or $\zeta_k = 0.05$ and $\eta = 0.02$ (simultaneous independent jump).
2. For $b = b_1, \dots, b_{10}$, calculate equation (42) where the theoretical survival probability $\mathbb{Q}(\tau_k > t_b)$ is calculated using current parameters of SSRJD.
3. Repeat Step 2 to minimize $\Psi\left(t_{b_{10}}, \boldsymbol{\beta}_k\right) = \sum_{i=1}^{10} \psi\left(t_{b_i}, \boldsymbol{\beta}_k\right)^2$ with the constraints $\psi(t_b, \boldsymbol{\beta}_k) \geq 0$ for all $b = b_1, \dots, b_{10}$ and $2\kappa_k\theta_k > \sigma_k^2$.

Regarding the correlation parameter $\rho_{C,R}^{jump}$ in equation (9), we set the parameter as the correlation $d\langle\lambda_C,\lambda_R\rangle(t)$ of SSRJD (7) equal to that of SSRD (5). When we adopt (i) simultaneous comonotone jump (SC-jump), that is, the jump size z_k is given as $z_k=\zeta_k z$ with the common exponential random number $z\sim \mathrm{Exp}(1)$, the correlation parameter $\rho_{C,R}^{jump}$ is given as

$$\rho_{C,R}^{jump}=\frac{\rho_{C,R}\sqrt{\sigma_C^2\theta_C+2\eta\zeta_C^2}\sqrt{\sigma_R^2\theta_R+2\eta\zeta_R^2}-2\eta\zeta_C\zeta_R}{\sigma_C\sigma_R\sqrt{\theta_C\theta_R}}. \tag{43}$$

When we adopt (ii) simultaneous independent jump (SI-jump), that is, the jump sizes z_C and z_R are independent, the correlation parameter $\rho_{C,R}^{jump}$ is given as

$$\rho_{C,R}^{jump}=\frac{\rho_{C,R}\sqrt{\sigma_C^2\theta_C+2\eta\zeta_C^2}\sqrt{\sigma_R^2\theta_R+2\eta\zeta_R^2}-\eta\zeta_C\zeta_R}{\sigma_C\sigma_R\sqrt{\theta_C\theta_R}}. \tag{44}$$

The calibrated parameters of SSRJD intensity are given in Table 4 for SC-jump and Table 5 for SI-jump.

Table 4 Calibration SSRJD default intensity with SC-jump

k	κ_k	θ_k	σ_k	$\lambda_k(0)$	ζ_k	η
Bank C	0.5681	0.0147	0.1293	0.0394	0.05	0.01
Firm R	0.4867	0.0058	0.0100	0.0021		

Table 5 Calibration SSRJD default intensity with SI-jump

k	κ_k	θ_k	σ_k	$\lambda_k(0)$	ζ_k	η
Bank C	0.5694	0.0139	0.1257	0.0394	0.05	0.02
Firm R	0.4829	0.0049	0.0100	0.0021		

2.6. Numerical comparison

We compare CVA of CDS with each year (1, 2, …, and 10 year) maturity under the following settings. The premium rate for each maturity sp_R is given as in Table 2. The notional amount NA is 100 million dollars. The loss rates given default for Bank C and Firm R are given as $\mathrm{LGD}_C=\mathrm{LGD}_R=0.6$ following the CDS market convention of 40% recovery rate. The number of paths for each simulation is given by 100,000.

2.6.1. Intensity model with/without simultaneous jump

We compare CVA of CDS under the following five settings and the results are in Figure 1. We can see that the CVA increases as the correlation coefficient, that is, CVA of No WWR < CVA of No Jump1 < CVA of No Jump2 when the maturity is long (9–10 years). For short maturities (less than 8 years), the difference in CVA of No Jump1 and that of No Jump2 is insignificant. We can also see that despite the correlation coefficient $\rho_{C,R}^{jump}$ of SC-Jump is adjusted to the larger correlation coefficient $\rho_{C,R}$ than that of SI-Jump, the CVA of SC-Jump is significantly smaller than that of SI-Jump.

1. No WWR: No jump and $\rho_{C,R} = 0$
2. No Jump1: $\rho_{C,R} = 0.3$
3. SI-Jump (simultaneous independent jump) $\rho_{C,R}^{jump} = 0.361$ is calculated from equation (44) with $\rho_{C,R} = 0.3$
4. No Jump2: $\rho_{C,R} = 0.4$
5. SC-Jump (simultaneous comonotone jump) $\rho_{C,R}^{jump} = -0.325$ is calculated from equation (43) with $\rho_{C,R} = 0.4$

Figure 1 CVA under intensity models

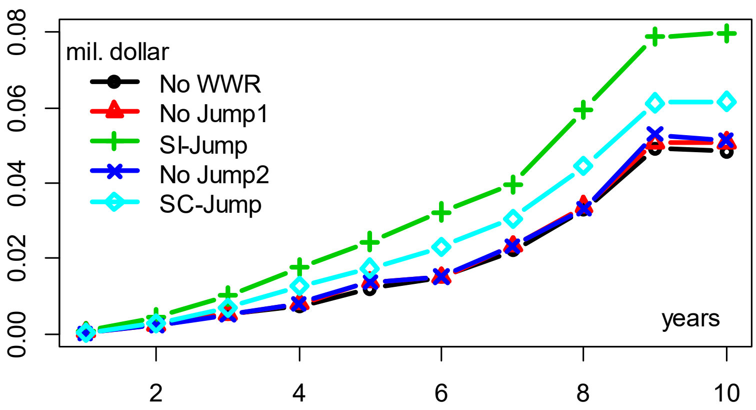

2.6.2. Copula approach with/without simultaneous jump

Focusing on simultaneous independent (SI-jump, $\rho_{C,R} = 0.3$ $<\rho_{C,R}^{jump} = 0.361>$) model for the intensity process of the counterparty and the reference firm, we compare CVA of CDS with Gaussian, Student's t ($\nu = 3$), Clayton, and Survival Gumbel copulas. Let $\rho_{C,R}^{copula}$ denote the copula-correlation between Bank C and Firm R. The parameter of the Clayton copula, α, is given by equation (32) with $\rho = \rho_{C,R}^{copula}$, and the parameter of Gumbel copula, γ, is given by equation (36) with $\rho = \rho_{C,R}^{copula}$.

Figure 2 plots the term structure for CVA of CDS with the four copulas: Gaussian, Student's t ($\nu = 3$), Clayton, and Survival Gumbel. Comparing with Figure 1, these figures show large impacts of the incorporation of copulas after the default of the counterparty. With the same $\rho_{C,R}^{copula} > 0$, CVA of Gaussian copula is much smaller than that of Student's t ($\nu = 3$), Clayton, or Survival Gumbel copula. It implies the Gaussian copula tends to underestimate the CVA, which is also indicated in Glasserman and Yang (2018). The Gaussian and Survival Gumbel copulas are reduced to independent copulas when $\rho_{C,R}^{copula} = 0$ while the Clayton copula is not defined for $\rho_{C,R}^{copula} = 0$. For a small (a) $\rho_{C,R}^{copula} = 0.1$, the CVA of CDS increases in the order Gaussian, Clayton, Survival Gumbel, and Student's t ($\nu = 3$). On the other hand, for a large (b) $\rho_{C,R}^{copula} = 0.5$, the CVA increases in the order Gaussian, Student's t ($\nu = 3$), Survival Gumbel, and Clayton.

Figure 2 CVA under copula approach with SI-Jump

(a) $\rho_{C,R}^{copula} = 0.1$ (b) $\rho_{C,R}^{copula} = 0.5$

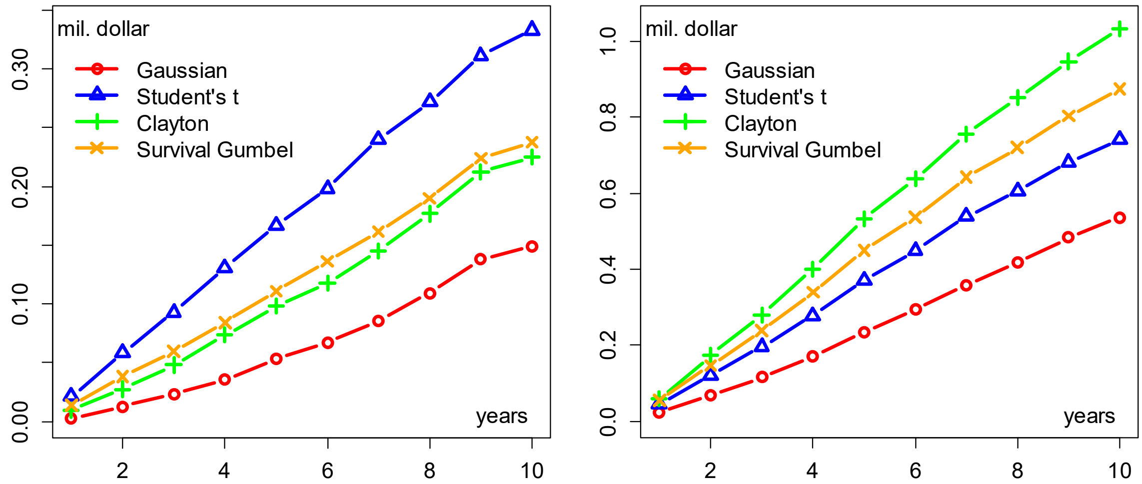

Figure 3 plots the CVA with 10 year maturity versus $\rho_{C,R}^{copula}$ focusing on SI-Jump with $\rho_{C,R} = 0.3$ ($\rho_{C,R}^{jump} = 0.361$). As Glasserman and Yang (2018) indicate, the Gaussian copula seems to underestimate the CVA relative to the values of Student's t ($\nu = 3$), Clayton, and Survival Gumbel copulas. We notice that the CVA of Student's t ($\nu = 3$) converges to larger values than that of Gaussian, Clayton, and Survival Gumbel copulas as $\rho_{C,R}^{copula} \to 0$. The result comes from the Student's t not converging to the independent copula as $\rho_{C,R}^{copula} \to 0$ while other copulas including Gaussian, Clayton, and Survival Gumbel copulas converge to the independent copula as $\rho_{C,R}^{copula} \to 0$. From Table 1, the lower tail dependence of Student's t ($\nu = 3$) copula converges to $2t_{\nu+1}\left(-\sqrt{\nu+1}\right) = 2t_4(-2) \cong 0.116$ as $\rho_{C,R}^{copula} \to 0$.

Figure 3 CVA of ten-year CDS under copula approach with SI-Jump versus $\rho_{C,R}^{copula}$

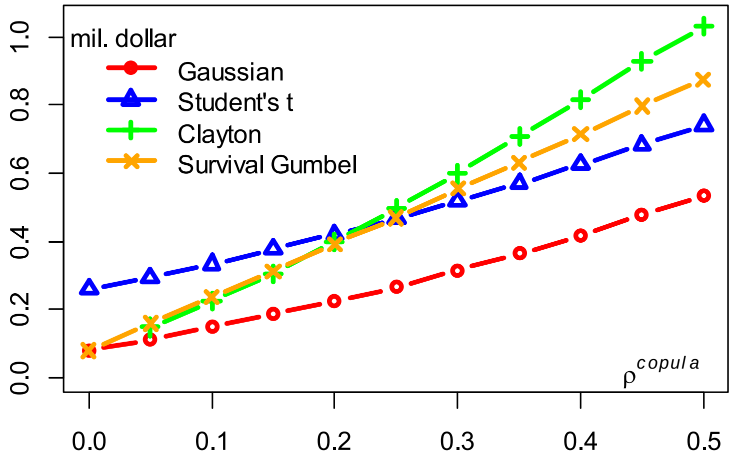

Comparing SI-Jump with SC-Jump in the copula approach, we see that the CVA of SI-Jump is larger than that of SC-Jump with Gaussian copula and other copulas for long maturities. On the other hand, the CVA of SC-Jump is larger than that of SI-Jump with Student's t ($\nu = 3$), Clayton, and Survival Gumbel copulas for short maturities. Figure 4 plots the difference of the CVA term structure between SC-Jump and SI-Jump. We see that the CVA of SI-Jump with most copulas is larger than that of SC-Jump with (a) $\rho_{C,R}^{copula} = 0.1$. On the other hand, for (b) $\rho_{C,R}^{copula} = 0.5$, the CVA of SC-Jump with Clayton, and Survival Gumbel copulas is larger than that of SI-Jump and the CVA of SC-Jump with Student's t ($\nu = 3$) copula for a maturity of less than eight years is larger than that of SI-Jump. The tail dependent copulas well capture the wrong-way risk represented by a very rare simultaneous comonotone jump.

Figure 4 Difference of CVA under copula approach between SC-Jump and SI-Jump

(a) $\rho_{C,R}^{copula} = 0.1$ (b) $\rho_{C,R}^{copula} = 0.5$

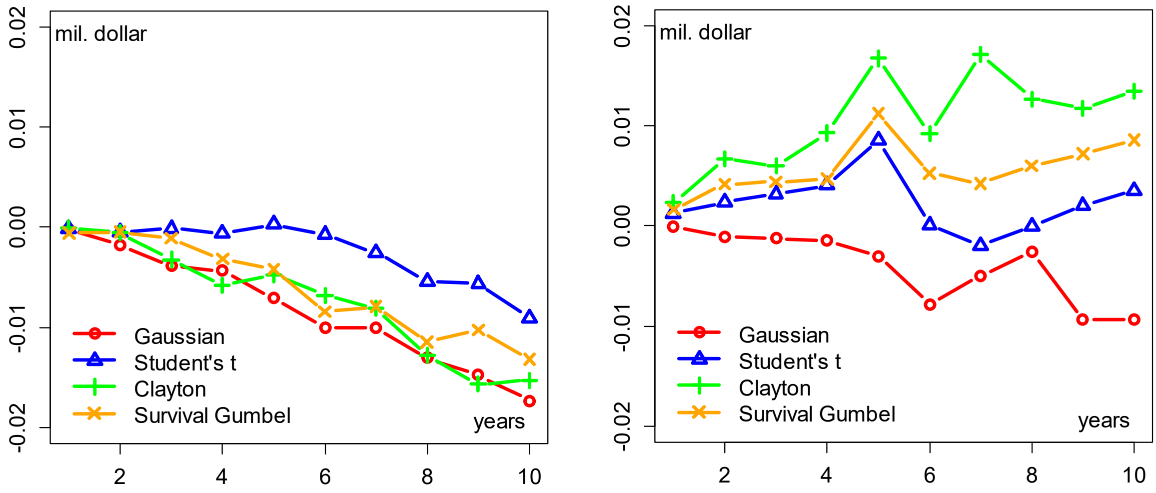

3. Conditional survival probabilities of SSRJD default intensities

This section shows how to derive the CDF of cumulative SRJD intensity.

3.1. Survival probability and characteristic function

The default intensity $\lambda_k(t)$ with SRJD (7) is one dimensional affine jump diffusion referred at equation (2.1) in Duffie, Pan, and Singleton (2000). Denoting the cumulative intensity from time *s* to *t* by

$$\Lambda_k(s,t) \equiv \int_s^t \lambda_k(y)dy, \tag{45}$$

and the expectation at time s under the risk-neutral measure $\mathbb{Q}$ by $\mathbb{E}_s^{\mathbb{Q}}[\cdot]$, both the survival probability $\mathbb{Q}(\tau_k > t|\tau_k > s) \equiv \mathbb{E}_s^{\mathbb{Q}}[\exp(-\Lambda_k(s,t))]$ and the characteristic function of the cumulative intensity $\phi_{k,s,t}(u) \equiv \mathbb{E}_s^{\mathbb{Q}}[\exp(\mathrm{i}u\Lambda_k(s,t))]$, $u \in \mathbb{R}$, $\mathrm{i} \equiv \sqrt{-1}$ are special cases of the moment generating function $M_{s,t}(\xi)$ where

$$M_{s,t}(\xi) \equiv \mathbb{E}_s^{\mathbb{Q}}[\exp(\xi\Lambda_k(s,t))], \tag{46}$$

The moment generating function $M_{s,t}(\xi)$ are represented by an exponential affine form $\exp(\alpha_J(s,t) + \alpha_D(s,t) + \beta(s,t)\lambda_k(s))$. As described on section 2.2 in Duffie, Pan, and Singleton (2000), the coefficients $\alpha_J(s,t)$, $\alpha_D(s,t)$, $\beta(s,t)$ have the following ordinal differential equations.

$$\frac{d\alpha_J(s,t)}{ds} = -\frac{\eta\zeta_k\beta(s,t)}{1-\nu_k\beta(s,t)}, \tag{47}$$

$$\frac{d\alpha_D(s,t)}{ds} = -\kappa_k\theta_k\beta(s,t), \tag{48}$$

$$\frac{d\beta(s,t)}{ds} = -\xi + \kappa_k\beta(s,t) - \frac{\sigma_k^2}{2}\beta^2(s,t), \tag{49}$$

where $\xi = -1$ for the survival probability $\mathbb{Q}(\tau_k > t|\tau_k > s)$ and $\xi = \mathrm{i}u$ for the characteristic function of the cumulative intensity $\phi_{k,s,t}(u)$.

The Riccati equation (49) is solved as

$$\beta(s,t) = \xi B(s,t), \tag{50}$$

where

$$B(s,t) = \frac{2\left(\exp\{h_\xi(t-s)\} - 1\right)}{2h_\xi + \left(\kappa_k + h_\xi\right)\left(\exp\{h_\xi(t-s)\} - 1\right)}, \tag{51}$$

$$h_\xi = \sqrt{\kappa_k^2 - 2\xi\sigma_k^2}. \tag{52}$$

See Appendix B for the derivation. Substituting equation (50) into (48) and integrating from s to t yields

$$\alpha_D(s,t) = \frac{2\kappa_k\theta_k}{\sigma_k^2}\log\frac{2h_\xi\exp\left\{\frac{\left(\kappa_k + h_\xi\right)(t-s)}{2}\right\}}{2h_\xi + \left(\kappa_k + h_\xi\right)\left(\exp\{h_\xi(t-s)\} - 1\right)}. \tag{53}$$

Substituting equation (50) into (47) and integrating from s to t yields

$$\alpha_J(s,t) = \frac{2\eta\zeta_k}{\sigma_k^2 - 2\kappa_k\zeta_k + 2\xi\zeta_k^2}\log\frac{2h_\xi\exp\left\{\frac{\left(\kappa_k + h_\xi - 2\xi\zeta_k\right)(t-s)}{2}\right\}}{2h_\xi + \left(\kappa_k + h_\xi - 2\xi\zeta_k\right)\left(\exp\{h_\xi(t-s)\} - 1\right)}. \tag{54}$$

The survival probability $\mathbb{Q}(\tau_k > t|\tau_k > s)$ for $\xi = -1$ is also solved by an exponential affine form as

$$\mathbb{Q}(\tau_k > t|\tau_k > s) = \exp\left\{\alpha_J(s,t) + \alpha_D(s,t) - B(s,t)\lambda_k(s)\right\}, \tag{55}$$

where h_1 in $\alpha_J(s,t)$, $\alpha_D(s,t)$, and $B(s,t)$ is given as

$$h_{-1} = \sqrt{\kappa_k^2 + 2\sigma_k^2}, \tag{56}$$

and equation (54) is represented as

$$\begin{aligned}&\alpha_J(s,t)_{|\xi=-1}\\ &= \frac{2\eta\zeta_k}{\sigma_k^2 - 2\kappa_k\zeta_k - 2\zeta_k^2}\log\frac{2h\exp\left\{\frac{(\kappa_k + h_{-1} + 2\zeta_k)(t-s)}{2}\right\}}{2h_1 + (\kappa_k + h_{-1} + 2\zeta_k)(\exp\{h_{-1}(t-s)\} - 1)}.\end{aligned} \tag{57}$$

The solution (55) of the survival probability is the same as that in Brigo and El-Bachir (2010).

The characteristic function of the cumulative intensity $\phi_{k,s,s+t}(u)$ is given as

$$\phi_{k,s,s+t}(u) = \exp\{\alpha_J(s, s+t) + \alpha_D(s, s+t) + \mathrm{i}uB(s, s+t)\lambda_k(s)\}, \tag{58}$$

where $h_{-\mathrm{i}u}$ in $\alpha_J(s,t)$, $\alpha_D(s,t)$, and $B(s,t)$ is represented as

$$h_{\mathrm{i}u} = \sqrt{\kappa_k^2 - 2\mathrm{i}u\sigma_k^2}, \tag{59}$$

and equation (54) is represented as

$$\alpha_J(s, s+t)_{|\xi=\mathrm{i}u} = \frac{2\eta\zeta_k}{\sigma_k^2 - 2\kappa_k\zeta_k + 2\mathrm{i}u\zeta_k^2} \log \frac{2h_{\mathrm{i}u}\exp\left\{\frac{(\kappa_k + h_{\mathrm{i}u} - 2\mathrm{i}u\zeta_k)t}{2}\right\}}{2h_{\mathrm{i}u} + (\kappa_k + h_{\mathrm{i}u} - 2\mathrm{i}u\zeta_k)(\exp\{h_{\mathrm{i}u}t\} - 1)}. \tag{60}$$

In the calculation of equation (58), we have to identify the single layer of Riemann surface related to the square root function of equation (59) and the log functions of equation (53) and (60).

3.2. Solutions to multivalued log functions

We define the regular log function by defining the Riemann surface, since the log function is a multivalued function in a complex space (see Rudin, 1987, for example).

3.2.1. Multivalued log function

We show the necessity to identify the Riemann surface of the log function to calculate the value of $\alpha_J(s,t)$ and $\alpha_D(s,t)$ properly. Figure 5 compares $\left|\exp\left(\alpha_J(s,t)\right)\right|$ between two cases; one is the log function with the proper Riemann surface (Riemann Considered) and the other without it (Riemann Unconsidered). Here we set $t - s =$ 10Yr and the SRJD parameters of Firm R in Table 4. The value of $\left|\exp\left(\alpha_J(s,t)\right)\right|$ without considering Riemann surface takes over 1 despite being supposed to be equal or less than 1. On the other hand, if the Riemann surface is taken into consideration, $\left|\exp\left(\alpha_J(s,t)\right)\right|$ takes equal or less than one properly.

Figure 5 Riemann surface considered versus unconsidered

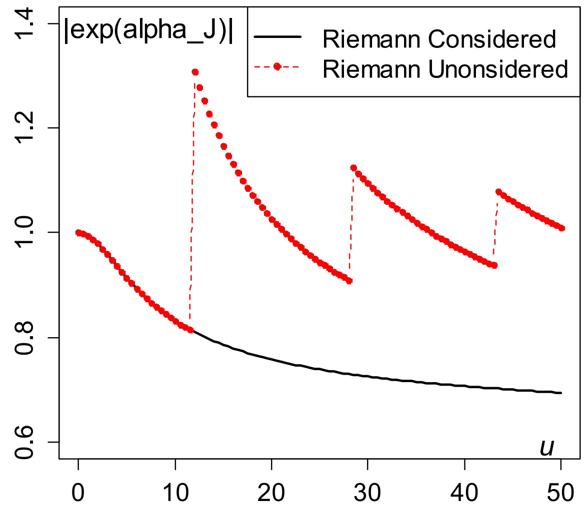

3.2.2. Effect of square-root functions

The square-root function as the h function in equation (59) is a bi-valued function in a complex space as

$$h_{\text{iu}} = \pm h_{\text{iu}}^{(+)}, h_{\text{iu}}^{(+)} = \sqrt{\frac{\kappa_k^2 + \sqrt{\kappa_k^4 + 4u^2\sigma_k^4}}{2}} - \mathrm{i}\sqrt{\frac{-\kappa_k^2 + \sqrt{\kappa_k^4 + 4u^2\sigma_k^4}}{2}}. \tag{61}$$

However, the bi-values have the same effect on the calculation, which is shown as

$$\begin{aligned}
&\frac{-2h_{\text{iu}}^{(+)}\exp\left\{\frac{\left(\kappa - h_{\text{iu}}^{(+)} - 2\mathrm{i}u\zeta\right)(t-t_0)}{2}\right\}}{-2h_{\text{iu}}^{(+)} + \left(\kappa - h_{\text{iu}}^{(+)} - 2\mathrm{i}u\zeta\right)\left(\exp\{-h_{\text{iu}}^{(+)}(t-t_0)\} - 1\right)} \\
&= \frac{-2h_{\text{iu}}^{(+)}\exp\left\{\frac{\left(\kappa - h_{\text{iu}}^{(+)} - 2\mathrm{i}u\zeta\right)(t-t_0)}{2}\right\}}{-2h_{\text{iu}}^{(+)} + \left(\kappa - h_{\text{iu}}^{(+)} - 2\mathrm{i}u\zeta\right)\left(\exp\{-h_{-\text{iu}}^{(+)}(t-t_0)\} - 1\right)} \frac{e^{h_{\text{iu}}^{(+)}(t-t_0)}}{e^{h_{\text{iu}}^{(+)}(t-t_0)}} \\
&= \frac{2h_{-\text{iu}}^{(+)}\exp\left\{\frac{\left(\kappa + h_{\text{iu}}^{(+)} - 2\mathrm{i}u\zeta\right)(t-t_0)}{2}\right\}}{2h_{\text{iu}}^{(+)} + \left(\kappa + h_{\text{iu}}^{(+)} - 2\mathrm{i}u\zeta\right)\left(\exp\{h_{\text{iu}}^{(+)}(t-t_0)\} - 1\right)}.
\end{aligned} \tag{62}$$

3.2.3. Solutions

Let $z(u)$ be a complex-valued function, $n(u)$ be the integer-valued function which indicates the number at which the Riemann surface passes the point $z = |z|$, $\mathrm{Log}(z(u))$ the principal value of the log function, and $\mathrm{Arg}(z(u))$ the argument of the principal value. Then the log function included in equations (53), (54), and (60) is defined as

$$\begin{aligned}\log(z(u)) &:= \mathrm{Log}(z(u)) + 2\pi \mathrm{i} n(u) \\ &= \mathrm{Log}(|z(u)|) + \mathrm{i}\left(\mathrm{Arg}(z(u)) + 2\pi n(u)\right).\end{aligned} \tag{63}$$

In practice, the implementation of $n(u)$ is the problem. Using a MATLAB or `signal` package on R, the function is given by `unwrap` and `Arg` functions applied to $z(u)$ in ascending order of u as

$$\mathrm{unwrap}(\mathrm{Arg}(z)) = \mathrm{Arg}(z(u)) + 2\pi n(u). \tag{64}$$

Guo and Hung (2007), Lord (2010), and Lord and Kahl (2010) also adopt the same approach in the evaluation of the derivative pricing under the Heston (1993) model.

Figure 6 plots the absolute value, real part, and imaginary part of the characteristic function $\phi_{k,s,s+t}(u)$ where the parameters of equation (7) are given as Firm R in Table 4.

Figure 6 The characteristic function

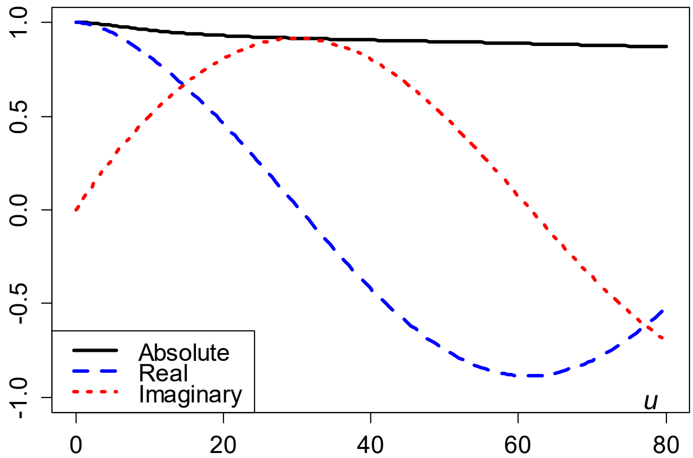

3.3. Fractional fast Fourier transform

3.3.1. Fourier inversion

Given the characteristic function $\phi(u) = \phi_{k,s,s+t}(u)$ of SSRJD cumulative intensity in equation (58), the density function $f(x)$ and the distribution function $F(x)$ are given by Fourier transforms as equations (65) and (66), respectively. Here, equation (65) can be derived using $\phi(u)^* = \phi(-u)$ because the density is a real valued function, where $\phi(u)^*$ is the complex conjugate of $\phi(u)$.

$$f(x) = \frac{1}{2\pi}\int_{-\infty}^{\infty} e^{-\mathrm{i}ux}\phi(u)du = \frac{1}{\pi}\mathrm{Re}\left[\int_{0}^{\infty} e^{-\mathrm{i}ux}\phi(u)du\right], \tag{65}$$

$$F(x) = \int_{-\infty}^{x} f(y)dy. \tag{66}$$

3.3.2. FRFT

Bailey and Swarztrauber (1991) propose fractional fast Fourier transform (FRFT) as an efficient computation for the discrete Fourier transform. The discrete Fourier transform for the vector $\boldsymbol{\phi} = (\phi_l)_{l=0}^{L-1}$ is defined as equation (67).

$$\int_{0}^{\infty} e^{-\mathrm{i}xu}\phi(u)du \approx \mathrm{FFT}_k[\boldsymbol{\phi}] := \sum_{l=0}^{L-1} e^{-\mathrm{i}\frac{2\pi}{L}kl}\phi_l. \tag{67}$$

Let ω be the grid of frequency, and χ be the grid of space, then the condition (68) should be satisfied.

$$\omega\chi = \frac{2\pi}{L}. \tag{68}$$

The right side of equation (68) corresponds to the exponent portion of the discrete Fourier transform of equation (67). The truncated wavenumber $u_{\max} = L\omega$ needs to be set to a value where the characteristic function is sufficiently small to reduce the truncation error (see Section 3.4.1). In addition, the number of sampling L should be larger than $2u_{\max}$ according to the sampling theorem. Since L and ω are determined by the constraints on the characteristic function and the sampling theorem, χ is determined through equation (68). A method free from this constraint condition is FRFT and is defined as equation (69).

$$\int_{0}^{\infty} e^{-\mathrm{i}xu}\phi(u)du \approx G(\boldsymbol{\phi}, \alpha) := \sum_{l=0}^{L-1} e^{-\mathrm{i}2\pi\alpha kl}\phi_l. \tag{69}$$

When $\alpha = 1/L$, it is equivalent to the discrete Fourier transform of equation (67). Equation (69) extends $\alpha = 1/L$ to an arbitrary rational number $\alpha = r/L$ ($r < L$, r and L are relatively prime). Since α is an arbitrary rational number and can be set so as to satisfy $\alpha = \omega\chi/2\pi$ after determining ω and χ independently, the constraint condition of equation (68) can be avoided. Expansion to an arbitrary rational number reduces to the discrete Fourier transform of $\bar{\boldsymbol{\phi}}$ obtained by sampling original data at regular intervals, as shown by equation (70).

$$\sum_{l=0}^{L-1} e^{-\mathrm{i}2\pi\alpha kl}\phi_l = \sum_{l=0}^{L-1} e^{-\frac{\mathrm{i}2\pi k(pl)r}{L}}\phi_{pl} = \sum_{l=0}^{L-1} e^{-\frac{\mathrm{i}2\pi kl}{L}}\phi_{pl} = \mathrm{FFT}_k[\bar{\boldsymbol{\phi}}]. \tag{70}$$

Here, p is a value determined so that the remainder dividing pr by L is 1 (ex. $r = 41$, $L = 1024$, $p = 25$). $\bar{\boldsymbol{\phi}}$ is obtained by sampling data every multiple of p and extending the sequence $\bar{\boldsymbol{\phi}}$ to length L by padding with zeros.

In this method, since ω and χ are not dependent on each other, we can reduce the calculation cost by adjusting them independently, which is not allowed for the conventional discrete Fourier transform because of the constraint condition (68). Bailey and Swarztrauber (1991) further represent the following method to reduce the calculation cost.

Since $2kl = l^2 + k^2 - (k-l)^2$, the right side of equation (69) is

$$\begin{aligned}\sum_{l=0}^{L-1} e^{-\mathrm{i}2\pi\alpha kl}\phi_l &= \sum_{l=0}^{L-1} \phi_l e^{-\pi\mathrm{i}\{l^2+k^2-(k-l)^2\}\alpha} \\ &= e^{-\pi\mathrm{i}k^2\alpha}\sum_{l=0}^{L-1} \phi_l e^{-l^2\pi\mathrm{i}\alpha}\, e^{(k-l)^2\pi\mathrm{i}\alpha} = e^{-\pi\mathrm{i}k^2\alpha}\sum_{l=0}^{L-1} y_l z_{k-l}.\end{aligned} \tag{71}$$

We remark that $y_l = \phi_l e^{-l^2\pi\mathrm{i}\alpha}$, $z_{k-l} = e^{(k-l)^2\pi\mathrm{i}\alpha}$. The outermost right hand side equation is the circular convolution. Let $\boldsymbol{y}$, $\boldsymbol{z}$ be $(y_l)_{l=0}^{L-1}$, $(z_l)_{l=0}^{L-1}$. In the case where z_{k-l} is periodic, it is calculated as a product of Fourier transforms as shown in equation (72).

$$\mathrm{FFT}_k\left[\left(\sum_{l=0}^{L-1} y_l z_{j-l}\right)_{j=0}^{L-1}\right] = \mathrm{FFT}_k[\boldsymbol{y}]\mathrm{FFT}_k[\boldsymbol{z}]. \tag{72}$$

The circular convolution in the most right-hand side of equation (71) is calculated by the inverse Fourier transform on the product of the Fourier transform calculated by equation (72) under the condition $z_{k-l} = z_{k-l+L}$. This condition is, however, violated in this case because $z_{k-l} = e^{(k-l)^2\pi\mathrm{i}\alpha} \neq e^{(k-l+L)^2\pi\mathrm{i}\alpha} = z_{k-l+L}$. To deal with this problem, Bailey and Swarztrauber (1991) employ vectors $\bar{\boldsymbol{y}} = (\bar{y}_l)_{l=0}^{2L-1}$ and $\bar{\boldsymbol{z}} = (\bar{z}_l)_{l=0}^{2L-1}$ by adding L new elements to $\boldsymbol{y}$ and $\boldsymbol{z}$. Following Chourdakis (2004), we apply weight vector $(0.5, 1, \ldots, 1, 0.5)$ to $\boldsymbol{y}$. The elements of $\bar{\boldsymbol{y}}$ are given as:

$$
\begin{aligned}
&\bar{y}_l = 0.5 * y_l, && l = 0, \\
&\bar{y}_l = y_l, && l = 1, \dots, L-2, \\
&\bar{y}_l = 0.5 * y_l, && l = L-1, \\
&\bar{y}_l = 0, && l = L, \dots 2L-1, \\
&\bar{z}_l = e^{l^2 \pi \mathrm{i} \alpha}, && l = 0, \dots, L-1, \\
&\bar{z}_l = e^{(2L-l)^2 \pi \mathrm{i} \alpha}, && l = L, \dots, 2L-1.
\end{aligned}
\tag{73}
$$

$\bar{\boldsymbol{y}}$ and $\bar{\boldsymbol{z}}$ satisfy the periodic condition because $\bar{z}_{k-l+2L} = e^{(2L-(k-l+2L))^2 \pi \mathrm{i} \alpha} = e^{(k-l)^2 \pi \mathrm{i} \alpha} = \bar{z}_{k-l}$. Using these vectors $\bar{\boldsymbol{y}}$ and $\bar{\boldsymbol{z}}$, the FRFT of is expressed as equation (75) using the inverse discrete Fourier transform defined as equation (74). The algorithm is shown in Appendix A.5.

$$
\mathrm{IFFT}_k[\bar{\boldsymbol{w}}] \coloneqq \frac{1}{2L} \sum_{j=0}^{2L-1} \bar{w}_j e^{\mathrm{i} 2\pi k j / 2L},
\tag{74}
$$

$$
\begin{gathered}
e^{-\pi \mathrm{i} k^2 \alpha} \sum_{j=0}^{L-1} \phi_j e^{-j^2 \pi \mathrm{i} \alpha} e^{(k-j)^2 \pi \mathrm{i} \alpha} = e^{-\pi \mathrm{i} k^2 \alpha} \, \mathrm{IFFT}_k[\bar{\boldsymbol{w}}], \\
\bar{\boldsymbol{w}} = \left(\mathrm{FFT}_j[\bar{\boldsymbol{y}}] \mathrm{FFT}_j[\bar{\boldsymbol{z}}] \right)_{j=0}^{2L-1}, \qquad 0 \le k < L.
\end{gathered}
\tag{75}
$$

3.4. Approximations

3.4.1. Truncation of the characteristic function

We set parameters of $x_{\max}$, $u_{\max}$, and L of FRFT with allowable truncation error of 10^{-6}. The maximum value of the cumulative default intensity $x = \Lambda_k(s,t)$, whose density is calculated as equation (65), is given by $x_{\max} = 15$ since $\exp(-15) \cong 10^{-6}$ where $\exp(-\Lambda_k(s,t))$ corresponds to the survival probability from time s to time t. The truncation value $u_{\max}$ of the characteristic function is calculated as $u_{\max} = \min\{u \mid |\phi(u)| < 10^{-6}\}$ depending on the residual time $T - \tau_C$ and the default intensity of the reference firm $\lambda_R(\tau_C)$ at the time of counterparty default τ_C. The number of grids L is given as $L = 2^{l_{\mathrm{sup}}}$ where $l_{\mathrm{sup}} = \min\{l \in \mathbb{Z}^+ : 2^l > 2u_{\max}\}$. With these parameters, the space grid is given as $\chi = x_{\max}/L$ and the wavenumber grid is given as $\omega = u_{\max}/L$.

Figure 7 plots the histogram of common logarithm of the absolute difference between analytical survival probabilities $\mathbb{Q}(\tau_R > t_m | \tau_C \in (t_{j-1}, t_j], \tau_R > t_j)$ given by equation (55) and the numerically integrated survival probabilities. Following equation (18), the numerically integrated survival probability is calculated as

$$\sum_{n=1}^{L} F_{\Lambda_R(T)-\Lambda_R(\tau_C)}(n\chi)e^{n\chi}(e^{\chi}-1)\,. \tag{76}$$

The survival probabilities are calculated for the paths with $\tau_R > \tau_C$ among 100,000 simulated paths with SI-Jump with $\rho_{C,R} = 0.3$ ($\rho_{C,R}^{jump} = 0.361$). The number of paths with $\tau_R > \tau_C$ is 19,281 in this case. We can see that the numerically integrated survival probability has the accuracy with small errors around 10^{-5}.

Figure 7 Histogram of common logarithm of absolute errors of survival probabilities

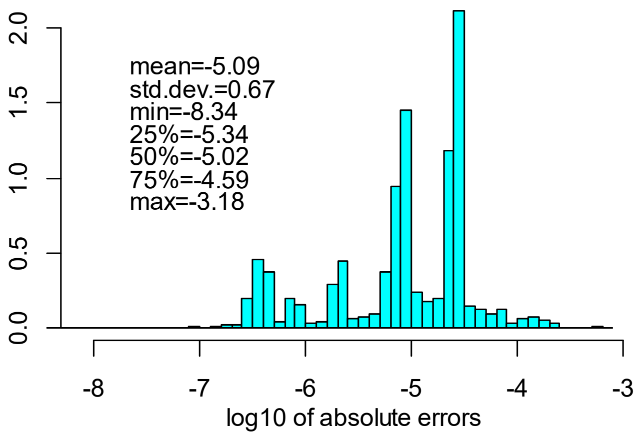

3.4.2. Approximation of intermediate conditional survival probabilities

Calculating $\mathbb{Q}(\tau_R > t | \tau_C \in (t_{j-1}, t_j])$ using equation (18) for all remaining time grids $t = t_l$ for $l = j+1, \ldots, m$ is time consuming. Hence, following Li (2001) capturing the dependence between each default until maturity by a copula in the valuation of the collateralized debt obligation, we only calculate $\mathbb{Q}(\tau_R > t_m | \tau_C \in (t_{j-1}, t_j])$ using equation (18) and approximate $\mathbb{Q}(\tau_R > t_l | \tau_C \in (t_{j-1}, t_j])$ for $l = j+1, \ldots, m-1$ as

$$\begin{aligned}\mathbb{Q}(\tau_R > t_l | \tau_C \in (t_{j-1}, t_j]) \\ \cong \exp\left[\log \mathbb{Q}(\tau_R > t_m | \tau_C \in (t_{j-1}, t_j]) \frac{\log \mathbb{Q}\left(\tau_R > t_l \middle| \lambda_R(t_j)\right)}{\log \mathbb{Q}\left(\tau_R > t_m \middle| \lambda_R(t_j)\right)}\right].\end{aligned} \tag{77}$$

Here, $\mathbb{Q}\left(\tau_R > t_l \middle| \lambda_R(t_j)\right)$ for $l = j+1, \ldots, m$ are calculated analytically using equation (55). The idea of this approximation comes from the interpolation by the mean default intensity.

Table 6 summarizes the average, standard deviation, and several percentiles with 0% (minimum), 1%, 10%, 25%, 50%, 75%, 90%, 99%, 100% (maximum) of error rates of the conditional exposure $V_{CDS}^{No\,CVA}(t_j)$ at $\tau_C \in (t_{j-1}, t_j]$ calculated as equation (2) for each copula including Gaussian, Student's t, Clayton, and Survival Gumbel. Each error rate is defined as $\{V_{CDS}^{Approx}(t_j) - V_{CDS}^{BF}(t_j)\}/V_{CDS}^{BF}(t_j)$, where $V_{CDS}^{Approx}(t_j)$ is the conditional exposure using the approximation of equation (77) and $V_{CDS}^{BF}(t_j)$ is the conditional exposure without the approximation. The conditional exposures are calculated for the paths with $\tau_R > \tau_C$ among 100,000 simulated paths with SI-Jump with $\rho_{C,R} = 0.3$ ($\rho_{C,R}^{jump} = 0.361$) and $\rho_{C,R}^{copula} = 0.1$. The number of paths with $\tau_R > \tau_C$ at least by one copula is 19,827 in this case. We can see that the approximation might underestimate slightly the precise value; however, the error is less than 6% even at one percentile. On the other hand, the calculation is about 86 times faster than a precise one. The precise calculation takes about two hundred hours over one week, on a standard spec computer.

Table 6 Summary statistics of error rates for each copula

	Gaussian	Student's t	Clayton	Sur. Gumbel
average	−0.46%	−0.59%	−0.77%	−0.74%
std. dev.	1.45%pt	3.30%pt	0.94%pt	1.40%pt
min	−175.56%	−36.41%	−7.65%	−64.98%
1%	−1.60%	−5.57%	−3.36%	−5.28%
10%	−1.26%	−2.46%	−2.20%	−2.39%
25%	−0.90%	−1.06%	−1.42%	−1.12%
50%	−0.27%	−0.05%	−0.41%	−0.20%
75%	0.00%	0.13%	0.00%	0.01%
90%	0.09%	0.30%	0.09%	0.12%
99%	0.26%	1.87%	0.26%	0.28%
max	16.73%	409.92%	4.13%	81.65%

4. Concluding remarks

We have analyzed several copulas to capture the wrong-way risk in CVA for CDS. While Brigo and Chourdakis (2009) and Brigo and Capponi (2010) focus on the shifted square root diffusion process without jump for the default intensities of the counterparty and the reference firm under a Gaussian copula to evaluate the CVA, we focus on the shifted square root jump diffusion (SSRJD) process for the default intensities under several copulas including Student's t, Clayton, and Survival Gumbel copula. After deriving the distribution function for the SSRJD cumulative default intensity by fractional fast Fourier transform (FRFT), we compare CVA of the four copulas. As shown in Glasserman and Yang (2018), the comparison implies the tail dependent copulas including Student's t, survival Gumbel, and Clayton copulas better capture the wrong-way risk than the Gaussian copula. In particular, the tail dependent copulas well capture the wrong-way risk represented by simultaneous jump with the very rare jump intensity.

We also show the concrete implementation of the copula approach using FRFT and validate the numerical errors and approximate intermediate conditional survival probabilities. The method also includes single-layered Riemann surface for the characteristic function of SSRJD cumulative intensity. The approach is widely applicable to option pricing with SSRJD underlying price movements and stochastic volatility model.

At the numerical analyses, we give the correlation parameter exogenously and do not calibrate them as in the preceding studies. If the counterparty and the reference firm are included in some traded CDO, the market implied correlation can be used for the correlation parameter.

Regarding the single name CDS, the settlements are concentrated on central counterparties as indicated in BIS statistics. Though in this paper we focused on the settlement with non-central counterparties, the analyses of CVA of CDS themselves can be extended and applied to the analyses on default funds of the central counterparties.

The proposed method in this paper is applicable to various fields. For example, it is of interest to study the valuation of CDS option, credit linked notes triggered by *n*-th to default, and derivative pricing with stochastic volatility of Affine jump diffusion (Carr *et al.*, 2003) with various types of dependencies.

References

Adachi, Tetsuya, and Yoshihiko Uchida, "Variation of Wrong-Way Risk Management and Its Impact on Security Price Changes," IMES Discussion Paper No.2015-E-12, Institute for Monetary and Economic Studies, Bank of Japan, 2015.

Bailey, David H., and Paul N. Swarztrauber, "The Fractional Fourier Transform and Applications," *SIAM Review*, **33**(3), 1991, pp.389–404.

Basel Committee on Banking Supervision (BCBS), "Basel III: Finalising Post-Crisis Reforms," Bank for International Settlements, 2017.

Bielecki, Tomasz R., Monique Jeanblanc, and Marek Rutkowski, *Credit Risk Modeling*, Osaka University CSFI Lecture Notes Series, Osaka University Press, 2009.

Black, Fischer, and Piotr Karasinski, "Bond and Option Pricing when Short Rates Are Lognormal," *Financial Analysts Journal*, **47**(4), 1991, pp.52–59.

Bo, Lijun, and Agostino Capponi, "Bilateral Credit Valuation Adjustment for Large

Credit Derivatives Portfolios," *Finance Stochastics*, **18**(2), 2014, pp.431–482.

Böcker, Klaus, and Michael Brunnbauer, "Path-Consistent Wrong-Way Risk," *Risk*, **27**(11), 2014, pp.48–53.

Brigo, Damiano, and Agostino Capponi, "Bilateral Counterparty Risk with Application to CDSs," *Risk,* **23**(3), 2010, pp.85–90.

———, and Kyriakos Chourdakis, "Counterparty Risk for Credit Default Swaps: Impact of Spread Volatility and Default Correlation," *International Journal of Theoretical and Applied Finance*, **12**(7), 2009, pp.1007–1026.

———, and Naoufel El-Bachir, "An Exact Formula for Default Swaptions' Pricing in the SSRJD Stochastic Intensity Model," *Mathematical Finance*, **20**(3), 2010, pp.365–382.

———, and Fabio Mercurio, *Interest Rate Models – Theory and Practice with Smile, Inflation and Credit* 2nd ed., Springer, 2006.

———, ———, and Andrea Pallavicini, *Counterparty Credit Risk, Collateral and Funding with Pricing Cases for All Asset Classes*, Wiley, 2013.

Carr, Peter, Hélyette Geman, Dilip B. Madan, and Marc Yor, "Stochastic Volatility for Lévy Processes," *Mathematical Finance*, **13**(3), 2003, pp.345–382.

Černý, Jakub, and Jiří Witzany, "A Copula Approach to Credit Valuation Adjustment for Swaps under Wrong-Way Risk," *Journal of Credit Risk*, **14**(1), 2018, pp.31–43.

Chourdakis, Kyriakos, "Option Pricing Using the Fractional FFT," *Journal of Computational Finance*, **8**(2), 2004, pp.1–18.

Duffie, Darrell, and Nicolae Gârleanu, "Risk and valuation of collateralized debt obligations," *Financial Analysts Journal*, **57**(1), 2001, pp.41–59.

———, Jun Pan, and Kenneth J. Singleton, "Transform Analysis and Asset Pricing for Affine Jump-diffusions," *Econometrica*, **68**(6), 2000, pp.1343–1376.

Glasserman, Paul, and Linan Yang, "Bounding Wrong-Way Risk in CVA Calculation," *Mathematical Finance*, **28**(1), 2018, pp.268–305.

Guo, Jia-Hau, and Mao-Wei Hung, "A Note on the Discontinuity Problem in Heston's Stochastic Volatility Model," *Applied Mathematical Finance*, **14**(4), 2007, pp.339–345.

Heston, Steven L., "A Closed-Form Solution for Options with Stochastic Volatility with Applications to Bond and Currency Options," *Review of Financial Studies*, **6**(2), 1993, pp.327–343.

Jarrow, Robert A., David Lando, and Fan Yu, "Default Risk and Diversification: Theory and Empirical Implications," *Mathematical Finance*, **15**(1), 2005, pp.1–26.

Lee, Jacky, and Luca Capriotti, "Wrong-way risk done right," *Risk*, **28**(9), 2015, pp.74–

79.

Leung, Seng Yuen, and Yue Kuen Kwok, "Credit Default Swap Valuation with Counterparty Risk," *The Kyoto Economic Review*, **74**(1), 2005, pp.25–45.

Li, David X., "On Default Correlation: A Copula Function Approach," *Journal of Fixed Income*, **9**(4), 2000, pp.43–54.

Lord, Roger, "Comment on: A Note on the Discontinuity Problem in Heston's Stochastic Volatility Model," *Applied Mathematical Finance*, **17**(4), 2010, pp.373–376.

———, and Christian Kahl, "Complex Logarithms in Heston-Like Models," *Mathematical Finance*, **20**(4), 2010, pp.671–694.

Mercurio, Fabio, and Minqiang, Li, "Jumping with Default: Wrong-Way-Risk Modeling for Credit Valuation Adjustment," **28**(11), 2015, pp.58–63.

Rosen, Dan, and David Saunders, "CVA the Wrong Way," *Journal of Risk Management in Financial Institutions*, **5**(3), 2012, pp.252–272.

Rudin, Walter, *Real and Complex Analysis*, 3rd edition, McGraw-Hill, 1987.

Schönbucher, Philipp J., and Dirk Schubert, "Copula-Dependent Default Risk in Intensity Models," Working Paper, Department of Statistics, Bonn University, 2001.

Appendix A. Implementation using R

A.1. Common procedures

The procedure to make the initial setting is implemented as the following codes in "initialSetting.R." The procedure includes a discounting factor from OIS market rates.

```
initialSetting <- function(tgtYr,settingFile,paraFile,oisFile,spRFile){
  makeDiscountFactor <- function(oneYearNum,matNum,oisFile){
    oisMat <- read.csv(oisFile);
    oisRate <- approxfun(oisMat);
    DF <- NULL;
    delta <- 1/oneYearNum;
    lessOneYearIdx <- 1:(oneYearNum-1);
    lessOneYear <- lessOneYearIdx*delta;
    DF[lessOneYearIdx] <- 1/(1+oisRate(lessOneYear)*lessOneYear);
    quarterNum <- oneYearNum/4;
    quarterNums <- seq(quarterNum,matNum,by=quarterNum);
    for(i in 4:length(quarterNums)){
      DF[quarterNums[i]] <-
(1-oisRate(quarterNums[i]*delta)/4*sum(DF[quarterNums[1:(i-1)]]))/(1+oisRate
(quarterNums[i]*delta)/4);
    }
    if(matNum>oneYearNum){
      quarterIdxs <- seq(oneYearNum,matNum-1,by=quarterNum);
      if(quarterNum>1){
        for(j in 1:(quarterNum-1)){
          zerob <- -log(DF[quarterIdxs])/(quarterIdxs*delta);
          zeroa <-
-log(DF[quarterIdxs+quarterNum])/((quarterIdxs+quarterNum)*delta);
          DF[quarterIdxs+j] <-
exp(-(zerob*(quarterNum-j)+zeroa*j)/quarterNum*delta*(quarterIdxs+j));
        }
      }
    }
    return(DF);
  }
  makeIntensityAdjustment <- function(psiYrs,tgtYr,oneYearNum){
    psi <- NULL;
    sy <- 0;
    for(i in c(1:nrow(psiYrs))[psiYrs[,"yrs"]<=tgtYr]){
      ey <- psiYrs[i,"yrs"];
      psi[(sy*oneYearNum+1):(ey*oneYearNum)] <- psiYrs[i,"psi"];
      sy <- ey;
    }
    return(psi);
  }
  setMat <- read.csv(settingFile);
  setting <- as.list(setMat[,"Value"]);
  names(setting) <- setMat[,"Names"];
  oneYearNum <- setting$oneYearNum;
  delta <- 1/oneYearNum;
  matNum <- tgtYr*oneYearNum;
  spRDat <- read.csv(spRFile);
  setting$prem <- spRDat[spRDat[,"Year"]==tgtYr,"Spread"]/10000*delta;
  paraMat <- read.csv(paraFile);
  psiIdxs <- grep("^psi",paraMat[,"Names"]);
  paraC <- as.list(paraMat[-psiIdxs,"ParaC"]);
  paraR <- as.list(paraMat[-psiIdxs,"ParaR"]);
```

```
  names(paraR) <- names(paraC) <- paraMat[-psiIdxs,"Names"];
  psiMat <- paraMat[psiIdxs,];
  yrs <- as.numeric(substr(psiMat[,"Names"],4,5))
  psiYC <- cbind(yrs,as.numeric(psiMat[,"ParaC"]));
  psiYR <- cbind(yrs,as.numeric(psiMat[,"ParaR"]));
  colnames(psiYR) <- colnames(psiYC) <- c("yrs","psi");
  paraR$eta <- setting$eta;
  setting$paraC <- paraC;
  setting$paraR <- paraR;
  setting$psiC <- makeIntensityAdjustment(psiYC,tgtYr,oneYearNum);
  setting$psiR <- makeIntensityAdjustment(psiYR,tgtYr,oneYearNum);
  setting$cumPsiR <- cumsum(setting$psiR)*delta;
  setting$DF <- makeDiscountFactor(oneYearNum,matNum,oisFile);
  setting$delta <- delta;
  setting$matNum <- matNum;
  return(setting);
}
```

The generating procedure of the default intensity and cumulative default probability is common among the default intensity model and the copula approach. The procedure is implemented as the following codes in "PathGeneratorCDS.R."

```
CptyDefaultPathJump <- function(setting,seed,simNum){
  paraC <- setting$paraC;
  psiC <- setting$psiC;
  paraR <- setting$paraR;
  psiR <- setting$psiR;
  eta <- setting$eta;
  delta <- setting$delta;
  matNum <- setting$matNum;
  rhoToRhoJump <- function(rhoCR,paraC,paraR,eta){
    zetaC <- paraC$zeta;
    zetaR <- paraR$zeta;
    sigC <- paraC$sigma;
    sigR <- paraR$sigma;
    varC <- sigC*sigC*paraC$theta+2*eta*zetaC*zetaC;
    varR <- sigR*sigR*paraR$theta+2*eta*zetaR*zetaR;
    if(JumpType==2){             ## Comonotone
return((rhoCR*sqrt(varC*varR)-2*eta*zetaC*zetaR) /
(sigC*sigR*sqrt(paraC$theta*paraR$theta)));
    }else if(JumpType==1){       ## Independent
      return((rhoCR*sqrt(varC*varR)-eta*zetaC*zetaR) /
(sigC*sigR*sqrt(paraC$theta*paraR$theta)));
    }
  }
  rho <- rhoToRhoJump(setting$rhoCR,paraC,paraR,eta,setting$JumpType);
  set.seed(seed);
  epsC <- matrix(rnorm(simNum*matNum),nrow=simNum,ncol=matNum);
  eps0 <- matrix(rnorm(simNum*matNum),nrow=simNum,ncol=matNum);
  epsR <- rho*epsC+sqrt(1-rho*rho)*eps0;
  xi <- matrix(rpois(simNum*matNum,eta*delta),nrow=simNum,ncol=matNum);
  z1 <- matrix(rexp(simNum*matNum),nrow=simNum,ncol=matNum);
  commonJump <- z1*xi;
  lambdaC <- lambdaR <- matrix(0,nrow=simNum,ncol=matNum+1);
  lambdaC[,1] <- paraC$lambda0;
  lambdaR[,1] <- paraR$lambda0;
  for(j in 1:matNum){
    lambdaC[,j+1] <- lambdaC[,j]+paraC$kappa*(paraC$theta-lambdaC[,j])*delta +
paraC$sigma*sqrt(lambdaC[,j]*delta)*epsC[,j]+paraC$zeta*commonJump[,j];
    lambdaC[lambdaC[,j+1]<0,j+1] <- 0;
    lambdaR[,j+1] <- lambdaR[,j]+paraR$kappa*(paraR$theta-lambdaR[,j])*delta +
paraR$sigma*sqrt(lambdaR[,j]*delta)*epsR[,j]+paraR$zeta*commonJump[,j];
```

```
    lambdaR[lambdaR[,j+1]<0,j+1] <- 0;
  }
  AdjLambdaC <- t(lambdaC[,-1])+psiC;
  lambdaR <- lambdaR[,-1];
  AdjLambdaR <- t(lambdaR)+psiR;
  cumPD_C <- 1-exp(-delta*t(apply(AdjLambdaC,2,cumsum)));
  cumPD_R <- 1-exp(-delta*t(apply(AdjLambdaR,2,cumsum)));
  if(setting$IntCop==0){  ## Default Intensity
    return(CptyDefaultPathInt(setting,simNum,cumPD_C,cumPD_R,lambdaR));
  }else{    ## Copula Approach
    return(CptyDefaultPathCop(setting,simNum,cumPD_C,cumPD_R,lambdaR));
  }
}
```

A.2. Procedures for the default intensity model

The procedure for sampling Cpty default paths under the default intensity model is implemented as the following codes in "PathGeneratorCDS.R" and is called in the function "CptyDefaultPathJump."

```
CptyDefaultPathInt <- function(setting,simNum,cumPD_C,cumPD_R,lambdaR){
  matNum <- setting$matNum;
  uC <- runif(simNum);
  uR <- runif(simNum);
  tauC <- matNum+1-apply(uC<cumPD_C,1,sum);
  tauR <- matNum+1-apply(uR<cumPD_R,1,sum);
  defIdxs <- as.logical((tauC<matNum) * (tauC<=tauR));
  defNum <- sum(defIdxs);
  resMat <- matrix(0,nrow=defNum,ncol=6);
  colnames(resMat) <- c("i","tauC","tauR","lambdaR","UC","UR_C");
  resMat[,"i"] <- c(1:simNum)[defIdxs];
  resMat[,"tauC"] <- tauC[defIdxs];
  resMat[,"tauR"] <- tauR[defIdxs];
  for(idx in 1:defNum){
    i <- resMat[idx,"i"];
    resMat[idx,"lambdaR"] <- lambdaR[i,tauC[i]];
    resMat[idx,"UC"] <- cumPD_C[i,tauC[i]];
    resMat[idx,"UR_C"] <- cumPD_R[i,tauC[i]];
  }
  return(resMat);
}
```

The procedures for the default intensity model are implemented as the following codes in "DefaultIntensity.R."

```
source("initialSetting.R");
source("PathGeneratorCDS.R");
source("SurviveProb.R")

ConditionalValue_CDS_Int <- function(setting, lambdaR_tauC, resNum, resNum,
tauC){
  paraR <- setting$paraR;
  PsiR <- setting$cumPsiR;
  delta <- setting$delta;
  survProb <- numeric(resNum+1);
  survProb[1] <- 1;
  for(j in 1:resNum){
    survProb[j+1] <- SurProb_SSRJD(paraR,PsiR,lambdaR_tauC,j,tauC,delta);
```

```
  }
  PD_R <- -diff(survProb);
  SurvPCurr <- survProb[-1];
  V <- setting$ DF[(tauC+1):(tauC+resNum)]/setting$DF[tauC]*(paraR$LGD*PD_R -
setting$prem*SurvPCurr);
  return(sum(V));
}

CVACalculator_CDS_Int <- function(tgtYr, simNum, seed, settingFile, paraFile,
oisFile){
  setting <- initialSetting(tgtYr,settingFile,paraFile,oisFile);
  setting$IntCop <- 0;
  cptyDefPath <- CptyDefaultPathJump(setting,seed,simNum);
  matNum <- setting$matNum;
  paraR <- setting$paraR;
  paraC <- setting$paraC;
  defNum <- nrow(cptyDefPath);
  futExp <- count <- numeric(matNum);
  simCVA <- numeric(defNum);
  for(idx in 1:defNum){
    tauC <- as.numeric(cptyDefPath[idx,"tauC"]);
    tauR <- as.numeric(cptyDefPath[idx,"tauR"]);
    if(tauC == tauR){
      curExp <- paraR$LGD*setting$notional;
    }else{
      resNum <-  matNum - tauC;
      lambdaR_tauC <- as.numeric(cptyDefPath[idx,"lambdaR"]);
      V <- ConditionalValue_CDS_Int(setting,lambdaR_tauC,resNum,tauC);
      curExp <- max(V,0)*setting$notional;
    }
    count[tauC] <- count[tauC] + 1;
    futExp[tauC] <- futExp[tauC] + curExp;
    simCVA[idx] <- setting$DF[tauC]*curExp*paraC$LGD;
  }
  return(list(defNum=defNum,simCVA=simCVA,futExp=futExp,count=count));
}
```

A.3. Procedures for the copula approach

The procedure for sampling Cpty default paths under the copula approach is implemented as the following codes in "PathGeneratorCDS.R" and is called in the function "CptyDefaultPathJump." The following `condCopSets(simNum,rho,nu)` function generate random vectors $(UC_j, URGa_j, URT_j, URClay_j, URSurGum_j)$ for $j = 1, \dots, simNum$ where the four pairs $(UC_j, URGa_j), (UC_j, URT_j), (UC_j, URClay_j)$, $(UC_j, URSurGum_j)$ have the same Kendall's tau with the Gaussian correlation of the parameter `rho`. The parameter `nu` denotes the degree of freedom parameter of the Student's t copula for the pair (UC_j, URT_j). In the function "condCopSets," the pair $(UC_j, URSurGum_j)$ is generated first following the latent variable θ_0 having a positive stable distribution with the stable parameter $1/\gamma$ and the skewness parameter 1. The three pairs $(UC_j, URGa_j), (UC_j, URT_j), (UC_j, URClay_j)$ are generated with the given UC_j.

```
condCopSets <- function(simNum,rho,nu){
  ## Survival Gumbel
  gam <- pi/(pi-2*asin(rho));
  V <- runif(simNum,max=pi);
  W <- rexp(simNum);
  th0 <- ((sin((gam-1)*V/gam)/W)^(gam-1))*sin(V/gam)/(sin(V)^gam);
  I <- matrix(runif(2*simNum),ncol=2);
  UC <- 1-exp(-((-log(I[,1])/th0)^(1/gam)));
  URSurGum <- 1-exp(-((-log(I[,2])/th0)^(1/gam)));
  ## Gaussian
  URGauss <- pnorm(rho*qnorm(UC)+sqrt(1-rho*rho)*rnorm(simNum));
  ## Student-t
  qtUC <- qt(UC,nu);
  URT <-
pt(rho*qtUC+sqrt(1-rho*rho)*sqrt((nu+qtUC*qtUC)/(nu+1))*rt(simNum,nu+1),nu);
  ## Clayton
  alpha <- 4*asin(rho)/(pi-2*asin(rho));
  URClay <- ((runif(simNum)^(-alpha/(alpha+1))-1)*UC^(-alpha)+1)^(-1/alpha);
  list(C=UC,RGa=URGauss,RT=URT,RCl=URClay,RSGu=URSurGum);
}

CptyDefaultPathCop <- function(setting,simNum,cumPD_C,cumPD_R,lambdaR){
  matNum <- setting$matNum;
  U <- condCopSets(simNum,setting$rhoCop,setting$nu);
  tauC <- matNum+1-apply(U$C<cumPD_C,1,sum);
  tauRGa <- matNum+1-apply(U$RGa<cumPD_R,1,sum);
  tauRT <- matNum+1-apply(U$RT<cumPD_R,1,sum);
  tauRCl <- matNum+1-apply(U$RCl<cumPD_R,1,sum);
  tauRSGu <- matNum+1-apply(U$RSGu<cumPD_R,1,sum);
  defIdxs <- as.logical(tauC<matNum);
  defNum <- sum(defIdxs);
  colNames <-
c("i","tauC","tauRGa","tauRT","tauRCl","tauRSGu","lambdaR","UC","UR_C");
  resMat <- matrix(0,nrow=defNum,ncol=length(colNames));
  colnames(resMat) <- colNames;
  resMat[,"i"] <- c(1:simNum)[defIdxs];
  resMat[,"tauC"] <- tauC[defIdxs];
  resMat[,"tauRGa"] <- tauRGa[defIdxs];
  resMat[,"tauRT"] <- tauRT[defIdxs];
  resMat[,"tauRCl"] <- tauRCl[defIdxs];
  resMat[,"tauRSGu"] <- tauRSGu[defIdxs];
  for(idx in 1:defNum){
    i <- resMat[idx,"i"];
    resMat[idx,"lambdaR"] <- lambdaR[i,tauC[i]];
    resMat[idx,"UC"] <- cumPD_C[i,tauC[i]];
    resMat[idx,"UR_C"] <- cumPD_R[i,tauC[i]];
  }
  return(resMat);
}
```

The procedures for the copula approach are implemented as the following codes in "CopulaApproach.R."

```
source("initialSetting.R");
source("PathGeneratorCDS.R");
source("SurviveProb.R")

ConditionalValue_CDS_Cop <- function(setting, lambdaR_tauC, resNum, tauC, UC,
UR_C){
  paraR <- setting$paraR;
  PsiR <- setting$cumPsiR;
  delta <- setting$delta;
  lsurvProb <- matrix(0,nrow=resNum+1,ncol=4);
```

```
  lsurvProb[resNum+1,] <- log(SurProb_SSRJD_Cops(setting, lambdaR_tauC, resNum,
tauC, UR_C, UC));
  lsurvProbIntMat <- log(SurProb_SSRJD(paraR, PsiR, lambdaR_tauC, resNum, tauC,
delta));
  for(j in 2:resNum){
    lsurvProbIntj <- log(SurProb_SSRJD(paraR, PsiR, lambdaR_tauC, j-1, tauC,
delta));
    lsurvProb[j,] <- lsurvProb[resNum+1,]*lsurvProbIntj/lsurvProbIntMat;
  }
  survProb <- exp(lsurvProb);
  PD_R <- -diff(survProb);
  SurvPCurr <- survProb[-1,];
  V <- setting$DF[(tauC+1):(tauC+resNum)]/setting$DF[tauC]*(paraR$LGD*PD_R -
setting$prem*SurvPCurr);
  return(apply(V,2,sum));
}

CVACalculator_CDS_Cop <- function(tgtYr, simNum, seed, rhoCop, settingFile,
corrFile, paraFile, oisFile,spRFile){
  setting <- initialSetting(tgtYr, settingFile, corrFile, paraFile, oisFile,
spRFile);
  setting$rhoCop <- rhoCop;
  setting$IntCop <- 1;
  cptyDefPath <- CptyDefaultPathJump(setting,seed,simNum);
  matNum <- setting$matNum;
  paraR <- setting$paraR;
  paraC <- setting$paraC;
  defNum <- nrow(cptyDefPath);
  count <- numeric(matNum);
  futExp <- matrix(0,nrow=matNum,ncol=4);
  simCVA <- matrix(0,nrow=defNum,ncol=4);
  for(idx in 1:defNum){
    tauC <- as.numeric(cptyDefPath[idx,"tauC"]);
    tauRGa <- as.numeric(cptyDefPath[idx,"tauRGa"]);
    tauRT <- as.numeric(cptyDefPath[idx,"tauRT"]);
    tauRCl <- as.numeric(cptyDefPath[idx,"tauRCl"]);
    tauRSGu <- as.numeric(cptyDefPath[idx,"tauRSGu"]);
    tauR <- c(tauRGa,tauRT,tauRCl,tauRSGu);
    curExp <- numeric(length(tauR));
    if(sum(tauC<tauR)){
      UC <-  as.numeric(cptyDefPath[idx,"UC"]);
      UR_C <-  as.numeric(cptyDefPath[idx,"UR_C"]);
      resNum <-  matNum - tauC;
      lambdaR_tauC <- as.numeric(cptyDefPath[idx,"lambdaR"]);
      V <- ConditionalValue_CDS_Cop(setting, lambdaR_tauC, resNum, tauC, UC,
UR_C);
      curExp <- V*setting$notional;
      curExp[curExp<0] <- 0;
    }
    curExp[tauC == tauR] <- paraR$LGD*setting$notional;
    curExp[tauC > tauR] <- 0;
    count[tauC] <- count[tauC] + 1;
    futExp[tauC,] <- futExp[tauC] + curExp;
    simCVA[idx,] <- setting$DF[tauC]*curExp*paraC$LGD;
  }
  return(list(defNum=defNum,simCVA=simCVA,futExp=futExp,count=count));
}
```

A.4. Survival probabilities

The procedures for survival probabilities are implemented as the following codes in

"SurviveProb.R." For survival probabilities until a short maturity, the calculation cost using FRFT, that is the number of L, skyrockets when the default intensity of the reference firm $\lambda_k(\tau_C)$ at the time of the counterparty default τ_C is small. Therefore, we do not use the characteristic function for the short residual maturity less than setting$midTerm. Instead, we interpolate the cumulative distribution function for the cumulative intensity until time $t <$ setting$midTerm using the distribution function at time setting$midTerm and the distribution function at the current time represented by the step function with 0 less than the current default intensity and 1 more than or equal to the intensity. We set setting$midTerm $= 0$ without using the interpolation in the main analysis.

```
source("CDFSRJD.R");

## Survival Probability with Shifted Square Root Jump Diffusion
SurProb_SSRJD <- function(paraR,PsiR,lambda_tauC,resNum,tauC,delta){
  mat <- resNum*delta;
  kappa <- paraR$kappa;
  sigma <- paraR$sigma;
  eta <- paraR$eta;
  h <- sqrt(kappa^2+2*sigma^2);
  kappah <- kappa+h;
  zeta <- paraR$zeta;
  as <- kappah+2*zeta;
  A <-
(2*h*exp(as*mat/2)/(2*h+as*(exp(h*mat)-1)))^(2*eta*zeta/(sigma^2-2*kappa*zet
a-2*zeta^2));
  B <- 2*(exp(h*mat)-1)/(2*h+kappah*(exp(h*mat)-1));
  C <-
(2*h*exp(kappah*mat/2)/(2*h+kappah*(exp(h*mat)-1)))^(2*kappa*paraR$theta/(si
gma^2));
  surProb <- A*C*exp(-B*lambda_tauC-PsiR[tauC+resNum]+PsiR[tauC]);
  return(surProb);
}

## Survival Probabilities with four copulas (with Jump)
## (Gaussian, Student’s t, Clayton, Surival Gumbel)
SurProb_SSRJD_Cops <- function(setting,lambda_tauC,resNum,tauC,UR_C,UC){
  delta <- setting$delta;
  mat <- resNum*delta;
  xmax <- setting$xmax;
  paraR <- setting$paraR;
  PsiR <- setting$cumPsiR;
  rho <- setting$rhoCop;
  midTerm <- setting$midTerm;
  if(mat < midTerm){
    temp <- uniroot(CharFuncIntSRJD, c(0,setting$uupper/(midTerm^2)),
para=paraR, lambdat=lambda_tauC, mat=midTerm, censorpoint=setting$ulower);
    umax <- temp$root;
    L <- 2^(ceiling(log(2*umax,2));
    pMid <- CDFIntSRJD(xmax,umax,L,paraR,lambda_tauC,midTerm);
    F <- numeric(L)+1;
    F[1] <- 0;
    F <- (F*(midTerm-mat)+pMid*mat)/midTerm;
  }else{
    temp <- uniroot(CharFuncIntSRJD, c(0,setting$uupper/(mat^2)), para=paraR,
```

```
lambdat=lambda_tauC, mat=mat, censorpoint=setting$ulower);
    umax <- temp$root;
    L <- 2^(ceiling(log(2*umax,2));
    F <- CDFIntSRJD(xmax,umax,L,paraR,lambda_tauC,mat);
  }
  uR <- 1-(1-UR_C)*exp(-seq(0,xmax,length=L));
  ## Gaussian
  xR_C <- (qnorm(UR_C)-rho*qnorm(UC))/sqrt(1-rho*rho);
  xR <- (qnorm(uR)-rho*qnorm(UC))/sqrt(1-rho*rho);
  CR_C <- (pnorm(xR)-pnorm(xR_C))/(1-pnorm(xR_C));
  PDs <- F[-L]*diff(CR_C);
  surPG <- sum(PDs);
  ## Student-t
  nu <- setting$nu;
  qtUC <- qt(UC,nu);
  coef <- sqrt((nu+1)/((nu+qtUC*qtUC)*(1-rho*rho)));
  xR_C <- coef*(qt(UR_C,nu)-rho*qtUC);
  xR <- coef*(qt(uR,nu)-rho*qtUC);
  CR_C <- (pt(xR,nu+1)-pt(xR_C,nu+1))/(1-pt(xR_C,nu+1));
  PDs <- F[-L]*diff(CR_C);
  surPT <- sum(PDs);
  ## Clayton
  alpha <- 4*asin(rho)/(pi-2*asin(rho));
  pdcopC <- function(u2,alpha){
    (UC^(-alpha-1))*((UC^(-alpha)+u2^(-alpha)-1)^(-1/alpha-1));
  }
  CR_C <- (pdcopC(uR,alpha)-pdcopC(UR_C,alpha))/(1-pdcopC(UR_C,alpha));
  PDs <- F[-L]*diff(CR_C);
  surPC <- sum(PDs);
  ## Survival Gumbel
  gam <- pi/(pi-2*asin(rho));
  pdcopSGu <- function(u2,gam){
    mlu1 <- (-log(1-UC));
    argCGu <- mlu1^gam+(-log(1-u2))^gam;
    CGu <- exp(-argCGu^(1/gam));
    1-CGu*(argCGu^(1/gam-1))*(mlu1^(gam-1))/(1-UC);
  }
  CR_C <- (pdcopSGu(uR,gam)-pdcopSGu(UR_C,gam))/(1-pdcopSGu(UR_C,gam));
  PDs <- F[-L]*diff(CR_C);
  surPSGu <- sum(PDs);
  surP <- cbind(surPG,surPT,surPC,surPSGu);
  names(surP) <- c("Gaussian","Student-t","Clayton","Survival Gumbel");
  surP <- surP * exp(-PsiR[tauC+resNum]+PsiR[tauC]);
  return(surP);
}
```

A.5. Distribution function for the cumulative SRJD intensity

The distribution function for the cumulative SRJD intensity is calculated as the following codes in "CDFSRJD.R." The procedures are implemented using the `signal` package which provides the `unwrap` function to make a single layer Riemann surface.

```
library(signal)

## Log vector of a complex vector zs
logVec <- function(zs){
  return(log(abs(zs))+1i*unwrap(Arg(zs)));
}

## Algorithm for the characteristic function of the integrated SRJD
```

```
CharFuncIntSRJD <- function(us, para, lambdat, mat, censorpoint){
  kappa <- para$kappa;
  sigma <- para$sigma;
  h <- sqrt(kappa^2-2*sigma^2*1i*us);
  kappah <- kappa+h;
  zeta <- para$zeta;
  as <- kappah-2*1i*zeta*us;
  A_J <- 2*h*exp(as*mat/2)/(2*h+as*(exp(h*mat)-1));
  alpha_J <- 2*para$eta*zeta*logVec(A_J)/(sigma^2-2*kappa*zeta +
2*zeta^2*1i*us);
  B <- 2*(exp(h*mat)-1)/(2*h+kappah*(exp(h*mat)-1));
  C_D <- 2*h*exp(kappah*mat/2)/(2*h+kappah*(exp(h*mat)-1));
  alpha_D <- 2*kappa*para$theta*logVec(C_D)/(sigma^2);
  phi <- exp(alpha_J+alpha_D+B*lambdat*1i*us);
  if(censorpoint != 0){return(abs(phi)-censorpoint);}
  else{return(phi);}
}

## Algorithm for the cumulative distribution function of the integrated SRJD
CDFIntSRJD <- function(xmax, umax, L, para, lambdat, mat){
  us <- seq(0,umax,length=L);
  phi <- CharFuncIntSRJD(us, para, lambdat, mat, 0);
  xgrid <- xmax/L;
  ugrid <- umax/L;
  piAlpha <- xgrid*ugrid/2;
  js <- seq(0,L-1);
  rjs <- seq(L,1);
  z1 <- exp(1i*piAlpha*js*js);
  z2 <- exp(1i*piAlpha*rjs*rjs);
  weight <- c(0.5,seq(1,1,length=L-2),0.5);
  fybar <- fft(c(phi*ugrid/z1*weight, seq(0,0,length=L)));
  fzbar <- fft(c(z1, z2));
  ifwbar <- fft(fybar*fzbar, inverse = TRUE)/(2*L);
  cdf <- cumsum(Re(ifwbar[1:L]/z1)*xgrid/pi);
  cdf[cdf<0] <- 0;
  cdf[cdf>1] <- 1;
  return(cdf);
}
```

Appendix B. Solution for a Riccati equation

Assume an ordinary differential equation

$$\frac{d\beta(s,t)}{ds} = -\frac{\sigma^2}{2}\beta(s,t)^2 + \kappa\beta(s,t) - \xi, \tag{B.1}$$

with the boundary condition

$$\beta(t,t) = 0. \tag{B.2}$$

Then the ordinary differential equation has a solution of

$$\beta(s,t) = \frac{2\xi(\exp\{h(t-s)\}-1)}{2h + (\kappa+h)(\exp\{h(t-s)\}-1)}, \tag{B.3}$$

where

$$h = \sqrt{\kappa^2 - 2\xi\sigma^2}. \tag{B.4}$$

Proof. Equation (B.1) is equivalent to:

$$\frac{d\beta(s)}{ds} = -\frac{\sigma^2}{2}(\beta(s) - \beta_1)(\beta(s) - \beta_2), \tag{B.5}$$

where

$$\beta(s) = \beta(s,t), \qquad \beta_1 = \frac{\kappa + h}{\sigma^2}, \qquad \beta_2 = \frac{\kappa - h}{\sigma^2}, \qquad h = \sqrt{\kappa^2 - 2\xi\sigma^2}. \tag{B.6}$$

Integrating equation (B.5) yields:

$$\begin{aligned} -\frac{\sigma^2}{2}(t - s) &= \int_s^t \frac{d\beta(u)}{(\beta(u) - \beta_1)(\beta(u) - \beta_2)} \\ &= \frac{1}{\beta_1 - \beta_2}\int_s^t \left\{\frac{1}{\beta(u) - \beta_1} - \frac{1}{\beta(u) - \beta_2}\right\} d\beta(u) \\ &= \frac{1}{\beta_1 - \beta_2}\left\{\ln\frac{\beta(t) - \beta_1}{\beta(s) - \beta_1} - \ln\frac{\beta(t) - \beta_2}{\beta(s) - \beta_2}\right\} \\ &= -\frac{\sigma^2}{2h}\left\{\ln\frac{\sigma^2\beta(s,t) - (\kappa + h)}{\sigma^2\beta(s,t) - (\kappa - h)}\left(\frac{\kappa - h}{\kappa + h}\right)\right\}. \end{aligned} \tag{B.7}$$

Rearranging equation (B.7) gives the solution (B.3).